Am J Nucl Med Mol Imaging 2013;3(1):57-70
www.ajnmmi.us /ISSN:2160-8407/ajnmmi1210003

Original Article

^{18}F-click labeling of a bombesin antagonist with an alkyne-^{18}F-ArBF$_3^-$: *in vivo* PET imaging of tumors expressing the GRP-receptor

Ying Li[1], Zhibo Liu[1], Curtis W Harwig[1], Maral Pourghiasian[2], Joseph Lau[2], Kuo-Shyan Lin[2], Paul Schaffer[3], Francois Benard[2], David M Perrin[1]

[1]*Chemistry Department, 2036 Main Mall, University of British Columbia, Vancouver, B.C., Canada V6T-1Z1;* [2]*BC Cancer Agency - Vancouver Centre, Centre for Functional Imaging, 600 West 10th Avenue, Vancouver, B.C. Canada V5Z-4E6;* [3]*Triumf, 4004 Wesbrook Mall, Vancouver, B.C. Canada V6T-2A3*

Received November 19, 2012; Accepted December 10, 2012; Epub January 5, 2013; Published January 15, 2013

Abstract: A clickable alkyne-modified arylborimidine is rapidly converted in 15 minutes to a highly polar ^{18}F-aryltrifluoroborate anion (^{18}F-ArBF$_3^-$) at high specific activity. Following labeling, the alkyne-^{18}F-ArBF$_3^-$ was conjugated to the peptide bombesin (BBN) within 25 minutes in a second step without need for prior work-up making this one-pot-two-step method easy, user-friendly, and generally applicable. Bombesin was chosen to provide functional PET images of prostate cancer xenografts in mice of which there are few. Whereas BBN is labeled to provide some of the first *in vivo* tumor images based on this technique, click-labeling is recognized for its generality and broad substrate scope. Hence these results are likely to be useful for click labeling most peptides and other biomolecules.

Keywords: ^{18}F-labeling, PET imaging, click chemistry, bombesin imaging

Introduction

PET imaging provides high resolution and dynamic images of target distribution and tracer clearance. Although many β^+-emitting isotopes have proven potentially useful, PET is most commonly associated with the use of ^{18}F. Indeed, the excellent nuclear properties of ^{18}F-fluorine which make it an ideal isotope for PET imaging include: i) a low β^+-emission energy for high resolution; ii) a near single decay path (> 97% β^+) such that nearly all decay events contribute to imaging signal; and iii) a moderate half-life (109.8 min) which is long enough for physiological perfusion yet short enough to minimize patient radiation exposure. Moreover the facile and on-demand ability to produce hundreds of milliCuries of ^{18}F-fluoride by ^{18}O(p,n)^{18}F in hospital cyclotrons account for its widespread use in clinical imaging [1].

Nevertheless, the poor reactivity of ^{18}F-fluoride ion in water along with a relatively short half-life makes aqueous ^{18}F-labeling of biomolecules difficult. To overcome the lack of reactivity in water, prosthetics are often synthesized under anhydrous conditions at high temperature prior to bioconjugation. Arylboronates capture ^{18}F-fluoride ion directly under aqueous conditions to afford a water-soluble, non-coordinating ^{18}F-labeled aryltrifluoroborate anion (^{18}F-ArBF$_3^-$) that is highly polar (log P < -4 for the ^{18}F-ArBF$_3^-$) [2-4]. Labeling proceeds rapidly at moderate temperature (20-40 °C) and at moderately acidic pH 2-3, making this method unique in its radiosynthetic attributes. Once the reaction is quenched to pH 7.5, the only stably isolable, radiolabeled product that remains is the ^{18}F-ArBF$_3^-$ [2]. Preliminary PET images of a biotinylated ^{18}F-ArBF$_3^-$ verified the *in vivo* stability of an ^{18}F-ArBF$_3^-$ as there was little if any apparent signal in bone [3]. The clinically trialed drug Marimastat was conjugated to a boronate and directly labeled at low specific activity ~0.1 Ci/μmol, to reveal tumor associated matrix metalloprotease activity in breast cancer xenografts [5, 6]. Furthermore, Lymphoseek™ was labeled with pendant fluorescent ^{18}F-ArBF$_3^-$

groups to provide sentinel lymph node images both with PET imaging and correlated fluorescence [7]. Most recently, we labeled RGD with a pendant ^{18}F-ArBF$_3^-$, albeit at low specific activity (Li *et al.*, Am J Nucl Med Mol Imaging 2013;3(1):(in press)).

Recently, one-pot-two-step click reactions (Cu^+-catalyzed and strain-promoted [2+3] cycloaddition reactions) are proving generalizable for labeling myriad peptides and other biomolecules [8-15]. Yet most click procedures still suffer from the drawback of needing dry conditions to produce a clickable ^{18}F-labeled prosthetic. In addition, the radioprosthetic can be quite hydrophobic, a characteristic that often results in blood retention and lower image quality. The unique and potential advantages of using an ^{18}F-ArBF$_3^-$ for labeling are: i) rapid radiosynthesis in aqueous conditions and ii) the production of a polar (anionic) ^{18}F-prosthetic whose hydrophilicity favors clearance. These advantages, coupled with the ability to use click chemistry for general peptide labeling would represent an important and broadly enabling advance.

Compared to other labeling methods that have been extensively explored, ^{18}F-ArBF$_3^-$ labeling is a relatively unexplored method that awaits validation in terms of producing tumor-specific images. Recently, we developed an alkyne-modified ^{18}F-ArBF$_3^-$ for a one-pot-two-step ^{18}F-labeling of RGD whereby no work-up is required between steps (Li et al. Am J Nucl Med Mol Imaging 2013;3(1):(in press)). Labeling proceeds in as little as 20 minutes while click conjugation requires another 20 minutes. Therefore the overall radiosynthesis time compares extremely favorably with other, recently reported click-type labeling that take up to 100 minutes or more [16, 17].

To further investigate the potential for labeling other peptides beyond RGD, here we have labeled bombesin, (BBN), at high specific activity (>1 Ci/μmol) for functional tumor imaging. BBN is a tetradecapeptide with high affinity (K_d ~ 1 nM) for the gastrin-releasing peptide receptor (GRPR) [18, 19], which is overexpressed on the cell surface of prostate [20], breast [21] lung [22], and some neuroendocrine tumors (NETs) [23]. Moreover, GRPR overexpression correlates with tumor differentiation [23] and enhanced mitogenic activity making it a useful target for diagnosing and grading specific neoplasms [24, 25]. Hence, BBN analogs represent important ligands for imaging GRPR-positive tumors *in vivo* in order to improve cancer diagnosis and prognosis [7, 26-28].

The N-terminal positions 1-3 of BBN tolerate bioconjugation to prosthetics, as evidenced by early reports on BBN-chelator conjugates labeled with ^{99m}Tc for use in SPECT [29-31]. Similar constructs chelate β^+-emitting metal ions [32] such as ^{64}Cu [33-36], and ^{68}Ga [37, 38], for PET imaging. Whereas chelation of β^+-radiometals offers great promise [39], demetallation has been observed with certain chelators. More stable chelates designed against demetallation often require much higher temperatures for labeling (80-90 °C) [40]. In terms of ^{18}F-labeling, BBN had been labeled via acylation of Lys-3 by ^{18}F-benzoate-NHS [41, 42], and more recently by direct nucleophilic aromatic displacement on an activated *N*-terminal benzamide at 130 °C [13, 18]. A recent report described strain-promoted two-step click ^{18}F-labeling using a *para*-^{18}F-benzylazide that reacts with a cyclooctyne-BBN conjugate yet no images were presented [43]. Recently, an elegant approach for direct ^{18}F-labeling employs a pendant ^{19}F-fluoro-di-*tert*-butylphenylsilane (SiFA) group that undergoes ^{19}F-^{18}F isotope exchange [13, 44-46]. Yet, when a ^{19}F-SiFA-BBN analog was labeled accordingly, no images were reported as uptake in tumor was lower than in blood [42]. A further challenge in GRPR imaging is that BBN agonists may also elicit mitogenic effects that would contraindicate their use in human patients. Hence there is great interest in imaging BBN *antagonists* that do not induce receptor signaling [27, 47, 48].

Here we develop an alkyne that is rapidly radiosynthesized in good yield, and which is condensed with an azido-BBN antagonist via a Cu^+-catalyzed [2+3] cycloaddition reaction. Three radiosyntheses are explicitly detailed in this work that delivered ^{18}F-labeled 2 at varying specific activities of 0.08 Ci/μmol, 0.24 Ci/μmol, and 1.9 Ci/μmol at EOS, (end of synthesis). Biodistribution and corroborating PET images at 1 Ci/μmol, with blocking controls showed tumor-specific uptake thereby validating this labeling method of which the critical components are identified in **Figure 1**.

Experimental section

Materials

Commercially available chemicals were purchased from Novabiochem, Sigma-Aldrich, Acros Organics, Oakwood or Alfa Aesar. Solvents were obtained from Fisher Scientific and used without further purification unless otherwise noted. The ^{18}F Trap & Release column (HCO_3^- form, ~ 10 mg) was purchased from ORTG, Inc., and C18 Sep-Pak cartridge (Vac 1cc, 50 mg) was obtained from Waters. TLC analysis was performed on aluminum-backed silica gel-60 plates from EMD Chemicals. Flash chromatography was carried out on SiliaFlash F60 (230-400 mesh) from SiliCycle. ESI-LRMS was performed on a Waters ZQ with a single quadrupole detector, attached to a Waters 2695 HPLC. ESI-HRMS were obtained on a Waters-Micromass LCT with a time-of-flight (TOF) detector. Alkyne-modified arylborimidine precursors were prepared as described previously (Li et al. Am J Nucl Med Mol Imaging 2013;3(1):(in press)).

Solid phase synthesis of BBN-N_3

2-Azidoacetyl-diethyleneglycol-[D-Phe^6]-BBN(6-13)NHEt was synthesized using an AAPPTEC Endeavor 90 peptide synthesizer via the N^{α}-Fmoc protocol starting with (3-[(ethyl-Fmoc-amino)methyl]indol-1-yl)acetyl AM resin. The Fmoc protecting group was removed using 20% piperidine in DMF. Couplings of the following protected amino acids, Fmoc-Leu-OH, Fmoc-His(Trt)-OH, Fmoc-Gly-OH, Fmoc-Val-OH, Fmoc-Ala-OH, Fmoc-Trp(Boc)-OH, Fmoc-Gln(Trt)-OH, Fmoc-D-Phe-OH, and Fmoc-PEG_2-OH, were carried out in NMP with 2.5 eq. of the noted amino acids activated *in situ* using HBTU in the presence of DIPEA (amino acid: HBTU: DIPEA 1:1:2). The last coupling was performed in DCM with 40 eq. of bromoacetic acid activated in situ using DIC (bromoacetic acid:DIC 2:1). The coupling reactions were monitored by Kaiser test, and repeated if required. After coupling, the resin was treated with 10 eq. of sodium azide in DMSO overnight to generate the azide functional group for use in click reaction. The peptide was then deprotected and cleaved from the resin using trifluoroacetic acid/tri-isopropylsilane/H_2O/phenol/thioanisole/ethanedithiol (81.5:1:5:5:5:2.5). The crude peptide was precipitated with cold Et_2O and collected by filtration and then purified by HPLC system via an isocratic condition (31.5% H_2O containing 0.1% TFA and 68.5 % CH_3CN containing 0.1% TFA) over the course of 25 min at a flow rate of 4.5 mL/min on a Phenomenex Luna C-18 semi-preparative column (250 mm × 10 mm, 5 mm) monitored on-line for UV absorption at 220 nm. The fractions of product with a retention time of 18.8 min were collected, pooled and followed by lyophilization. Overall yield: 41% (> 97% purity). ESI-MS: $[M+1]^+$: 1227.0, $[M+Na]^+$: 1249.0.

BBN-ArBF_3^-

(3) BBN-N_3 (5.4 mg, 4.4 μmol), alkyne-ArBF_3 (2) (5.5 mg, 17.2 μmol), and DIPEA (10 μL, 57.4 μmol) in DMF (200 μL) and H_2O (25 μL) was added with 400 mM sodium ascorbate (470 μL) and 100 mM $CuSO_4$ (270 μL). The reaction was shaken at room temperature for 2 hr. and then injected to HPLC for purification to give the desired product. Yield: 1.4 mg, 22%. HRMS: calcd. for $C_{68}H_{88}BN_{18}O_{14}F_6^-$: 1505.6725, found: 1505.6752. HPLC chromatography was performance on the Agilent 1100 HPLC system equipped with an auto-injector, a fraction collector and a diode array detector. For preparation (t_R= 14.5 min): column: Agilent Eclipse XDB-C18 5 mm 9.4 x 250 mm column, flow rate: 3 mL/min, column temperature: 50 °C, HPLC gradient: solvent A: 0.04 M NH_4HCO_2, solvent B: CH_3CN, 0 min to 3 min, 0% B to 5% B, 3 min to 6 min, 5% B to 20% B, 6 min to 12 min, 20% B to 50% B, 12 min to 15 min, 50% B to 100% B, 15 min to 15.5 min, 100% B to 95% B, 15.5 min to 16 min, 95% B to 5% B, 16 min to 17 min, 5% B. For analysis (t_R = 20.7 min), column: Phenomenex Jupiter 10μ C18 300A 4.6 × 250 mm column, flow rate: 1 mL/min, column temperature: 50 °C. HPLC gradient: solvent A: 0.04 M NH_4HCO_2, solvent B: CH_3CN, 0 min to 5 min, 0% B to 5% B, 5 min to 10 min, 5% B to 20% B, 10 min to 20 min, 20% B to 50% B, 20 min to 25 min, 50% B to 100% B, 25 min to 28 min, 100% B to 95% B, 28 min to 30 min, 95% B to 5% B, 30 min to 32 min, 5% B. Following collection, the sample was lyophilized.

General radiosynthetic methods

^{18}F-fluoride ion was obtained from the bombardment of ^{18}O-H_2O with 12.5 MeV protons in a niobium target and transferred to the hot cell through a pre-activated anion exchange col-

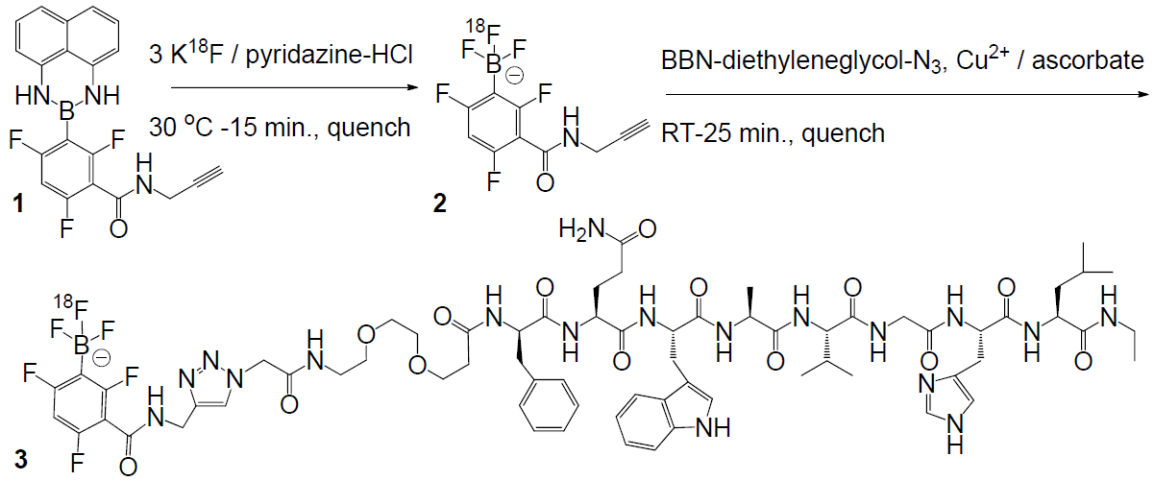

Figure 1. Radiosynthetic scheme for rapid one-pot-two-step ^{18}F-labeling of BBN following conversion of borimidine 1 to alkyne-modified ^{18}F-ArBF$_3^-$.

umn (HCO_3^- or Cl^- form). Following quench, the crude reaction was injected onto an analytical RP C18 HPLC column connected to an Agilent 1200 series with a viable wavelength detector and Bioscan radioactivity NaI detector. In all cases, a Phenomenex Jupiter 10m C18 300Å 4.6 mm × 250 mm column was used with a flow rate: 1 mL/min at room temperature. The HPLC gradient used was: solvent A: 0.04 M NH_4HCO_2, solvent B: CH_3CN, 0 min to 5 min, 0% B to 5% B, 5 min to 10 min, 5% B to 20% B, 10 min to 20 min, 20% B to 50% B, 20 min to 25 min, 50% B to 100% B, 25 min to 28 min, 100% B to 95% B, 28 min to 30 min, 95% B to 5% B, 30 min to 32 min, 5% B to 0.5% B.

Radiosyntheis 1 (for ex vivo biodistribution study)

^{18}F-Fluoride ion was trapped on an anion exchange column (ORTG, HCO_3^- form) and eluted with 4 mg/mL $NaClO_4$ solution (0.3 mL) into a glass V-vial containing CH_3CN (0.5 mL). The ^{18}F-fluoride ion solution (136.9 mCi at EOB) was concentrated under He flow at 110 °C. The dry ^{18}F-fluoride ion was then resuspended in 0.127 M KHF_2 (5 μL). The freshly prepared ^{18}F-fluoride ion solution (2 μL, 23.7 mCi at 23 min at a specific activity of 0.047 Ci/μmol), was added to the mixture of 1 (100 nmol) in THF (4 μL) and conc. HCl (0.5 μL). The reaction was incubated at room temperature for ~ 20 min and then quenched with 5% NH_4OH in 50% aqueous EtOH (10 μL) at 45 min The entire quenched reaction (14.7 mCi at 49 min) was transferred to a mixture of BBN-N_3 (100 nmol) in THF (5 μL) and freshly prepared 0.75 M sodium ascorbate (4 μL). Then freshly prepared 0.25 M $CuSO_4$ solution (2 μL) was added and the click reaction was then left at room temperature for ~ 30 min The reaction (8.88 mCi at 84 min) was diluted with 5% NH_4OH in 50% aqueous EtOH (70 μL) and HPLC purified. The fraction containing the desired product (2.99 mCi at 104 min) was collected manually, diluted with H_2O (15 mL), and loaded to a preactivated Waters C18 Sep-Pak cartridge (100 mg). The cartridge was further washed with H_2O (10 mL) and eluted with EtOH fractions (50 μL/fraction). The desalted product (2.17 mCi at 118 min) was diluted with saline buffer (2 mL) and expedited for biodistribution studies (specific activity calculated to be ~ 0.077 Ci/μmol).

Radiosynthesis 2 (for animal PET imaging)

^{18}F-Fluoride ion (6 μL, 33.1 mCi at EOB) was added to an eppendorf tube containing 1 (30 nmol) and ^{19}F-fluoride ion (30 nmol, in the form of KHF_2) in DMF (5 μL) and 0.55 M solution of pyridazine HCl buffer (pH 1.8) in aqueous DMF (2 μL). The reaction was then dried in a desiccator under a vacuum of 0.1 mm Hg connected to a glass column 2 cm × 10 cm filled with 3Å molecular sieves to trap any evolved ^{18}F-HF. After 20 min, the vacuum was released and the reaction was dissolved in 5% NH_4OH in 50% aq. EtOH (5 μL) containing BBN-N_3 (100 nmol), followed by the addition of freshly made 0.6 M sodium ascorbate (4 μL) and 0.2 M $CuSO_4$ (2

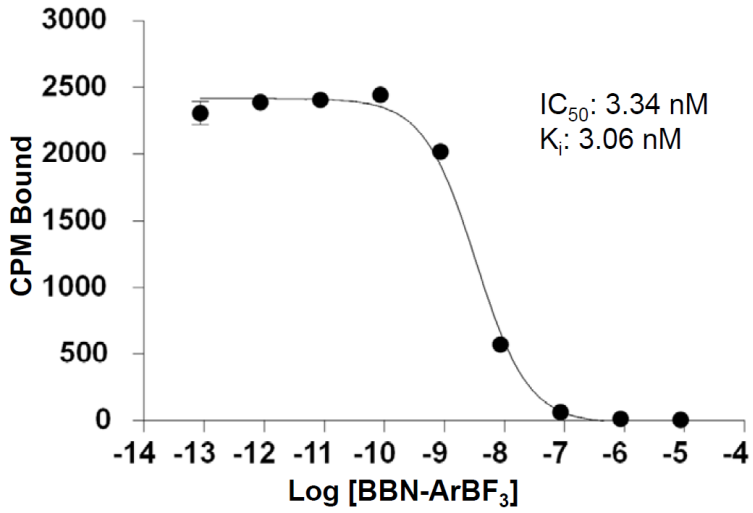

Figure 2. The binding constant (K_i) of BBN-$ArBF_3^-$ was determined by performing a competitive binding assay using ^{125}I-Tyr-BBN (Perkin Elmer) on PC-3 human prostate adenocarcinoma cells.

μL). After 25 min at room temperature, the reaction was quenched with 5% NH_4OH in 50% aqueous EtOH (100 μL) and the entire reaction (8.4 mCi) was HPLC purified. The desired product (2.87 mCi at 80 min) was collected manually in 3 fractions which were diluted with H_2O (20 mL) and loaded onto a preactivated Waters C18 Sep-Pak cartridge (50 mg, 1 cc). The cartridge was washed with H_2O (10 mL). The radiotracer was then released with EtOH into two major fractions (50 μL per fraction). The two major fractions were combined and diluted with saline buffer (1.9 mL) for delivery (2.2 mCi, specific activity calculated to be ~1.9 Ci/μmol at time of packaging) signifying an *isolated* radiochemical yield of 6% (not corrected for decay). Independent measurement of the specific activity by HPLC based on reinjection of radiolabeled 3 when recorded at 220 nm gave less reliable data including the appearance of another non-radiolabeled peak, likely representing conjugation to the unlabeled arylboronates, which could reduce effective specific activity to 0.5-1 Ci/μmol.

Radiosynthesis 3 (for plasma stability test)

^{18}F-Fluoride ion (106.5 mCi at EOB) in an eppendorf tube was concentrated in the desiccator under vacuum ~ 22 min to give a white pellet. KHF_2 (2 μL, 0.127 M, 254 nmol) was added to (82.5 mCi at 35 min) to bring the SA of the ^{18}F-fluoride ion to 0.162 Ci/μmol and this solution was added to 1 (100 nmol) in THF (5 μL). To initiate the labeling, conc. HCl (0.5 μL) was added to the reaction. The reaction mixture was incubated at room temperature for ~ 20 min and then quenched with 5% NH_4OH in 50% aqueous EtOH (10 μL) containing BBN-N_3 (100 nmol). To the quenched reaction (64.2 mCi at 59 min) was added with freshly prepared 0.6 M sodium ascorbate (6 μL) and 0.2 M $CuSO_4$ (3 μL). After 25 min, the reaction was quenched with 5% NH_4OH in 50% aqueous EtOH (200 μL). Approximately 80 μL of the diluted crude (21 mCi at 107 min) was HPLC purified. The desired product (5 mCi at 138 min) was collected and desalted by solid phase extraction described above. The two EtOH fractions (total 4.27 mCi at 150 min in 100 μL) were combined and directly used for the plasma stability test (SA 0.24 Ci/μmol).

Plasma stability test

BBN-^{18}F-$ArBF_3^-$ (4.27 mCi) in EtOH (100 μL) was diluted in saline buffer (2 mL). For each assay, the saline solution (200 μL) was mixed with plasma (200 μL), incubated at 30 °C for 0, 15, 30, 60 and 120, and quenched by the addition of 75% aqueous CH_3CN (400 μL). The resulting mixture was vortexed and centrifuged at 13 krpm for 20 min. The supernatant was isolated, filtered, and analyzed by HPLC for further analysis shown below the percent converted to other products was plotted on the graph below and is similar to serum stabilities seen for bombesin.

Biodistribution studies and PET imaging

The animal protocol used in the animal studies was approved by the Institutional Animal Care Committee of the University of British Columbia and was performed in compliance with the Canadian Council on Animal Care Guidelines. 6-8 weeks old male nude mice purchased from Simonsen laboratories were used for animal studies. ^{18}F-Labeled 3, at low specific activity, was imaged in two healthy mice without tumors and a biodistribution study was conducted on these mice. For induction of tumor xenografts,

male nude mice were inoculated subcutaneously with 5 x 10^6 PC-3 tumor cells on each shoulder. PC-3 tumor cells were freshly expanded in sterilized PBS/matrigel mixture prior to inoculation. The tumors were allowed to grow 3-4 weeks to reach a suitable size (5-7mm in diameter) for biodistribution studies and PET/CT imaging. For biodistribution studies in mice with tumors, once anesthetized, 10-20 μCi of tracer was injected via the tail vain. To determine the specificity of the *in vivo* uptake in receptor positive tissues, 100 μg of unlabeled BBN as a blocking agent was pre-injected (10 min) to an additional group of mice. Mice were humanely euthanized by carbon dioxide and dissected 1 hour post-injection. Tissues of interest were collected, rinsed, dried and counted in a gamma counter (Cobra-II Auto Gamma, Canberra Packard Canada). The tissue weight and associated cpm (counts per min) were used to calculate the percentage of injected dose per gram of tissue (%ID/g). PET imaging was performed in the Siemens Inveon multimodality small animal PET/CT scanner. For Dynamic PET/CT imaging, tumor-bearing animals were anaesthetized using 1.5-2% isoflurane and the tail vein was catheterized. Mice were placed onto the imaging bed while anaesthetized. A 10 minute CT attenuation scan followed by a 60 minute Dynamic PET scan was carried out. 100 μCi of radiotracer was injected via catheter 30 seconds after PET acquisition started. For blocking studies, 100 μg of unlabeled BBN was injected prior to the CT attenuation. Mice were euthanized after scanning. The list-mode data was histogrammed at various time intervals, and reconstructed by an iterative reconstruction algorithm (3D OSEM/MAP) using the Inveon Acquisition Workplace Software (Siemens), applying normalization, dead time, random and attenuation correction. The attenuation correction map was obtained from the CT scan data.

Results

Briefly, carboxytrifluorophenylboronic acid, the precursor of an *in-vivo* stable $ArBF_3^-$, was protected with diaminonaphthalene (dan) [49, 50] and then converted to the propargylamide providing the required alkyne functionality (Li *et al*., Am J Nucl Med Mol Imaging 2013;3(1):(in press)). In contrast to previous reports where tetraphenylpinacol (tpp) was used to protect the boron, we chose the more acid-labile (dan), which is released more rapidly to provide higher chemical/radiochemical yields of the $ArBF_3^-$. Compound 1 (**Figure 1**) therefore represents a shelf-stable "radiosynthon" precursor that can be readily labeled under aqueous conditions as an ^{18}F-$ArBF_3^-$ 2, which then undergoes Cu^+-mediated conjugation, all in one pot, in less than 1 hour.

Here we feature click labeling of a truncated octapeptide bombesin analog [D-Phe^6]-BBN(6-13)NHEt (BBN) that was chosen because it is an antagonist for the GRPR and does not elicit any mitogenic response upon binding [47, 51]. An azide was affixed to the *N*-terminal diethyleneglycol (deg) carboxamide linker. Unlabeled alkyne-$ArBF_3^-$ 2 was prepared according to standard protocols [52-54]. With significant quantities of unlabeled 2 in hand, conditions for Cu^+-catalyzed conjugation were optimized in terms of reaction time, Cu^+-concentration, and the minimum amount of excess N_3-BBN needed to convert 2 to 3 in high yield (>95%). Competition binding assays were performed using GRPR-expressing PC3 cells to verify that 3 exhibited a K_i of ~3 nM (**Figure 2**), consistent with other BBN derivatives.

Three different radiosyntheses detailed herein involved relatively low levels of ^{18}F-activity (~ 50 mCi) and gave reproducibly quantitative (> 95%) conversion of 2 to produce 3 with an overall isolated radiochemical yield of 20±10% (n=3, **Figure 3**, not decay corrected). In each case, the crude reaction was applied to an analytical HPLC column and the *crude* radiotraces are provided in **Figure 3**, which demonstrates reproducibly excellent radiochemical purity that elutes in essentially a single, easily collected, radiolabeled peak corresponding to the labeled bombesin (note that incorporated ^{18}F-fluoride ion elutes at 2-4 minutes). A small peak eluting ~1 min prior to the desired peak in **Figure 3C** was attributed to a minor unidentified labeled product. In each case, the HPLC-purified radiolabeled material was checked for radiochemical purity (see supporting information for radiotraces).

Plasma stability assays on radiochemically pure material showed high stability with ~ 10% degradation and/or solvolytic defluoridation observed after 2 hours (**Figure 4**). This is compares slightly less favorably to other plasma stability studies of labeled bombesin [18, 55]

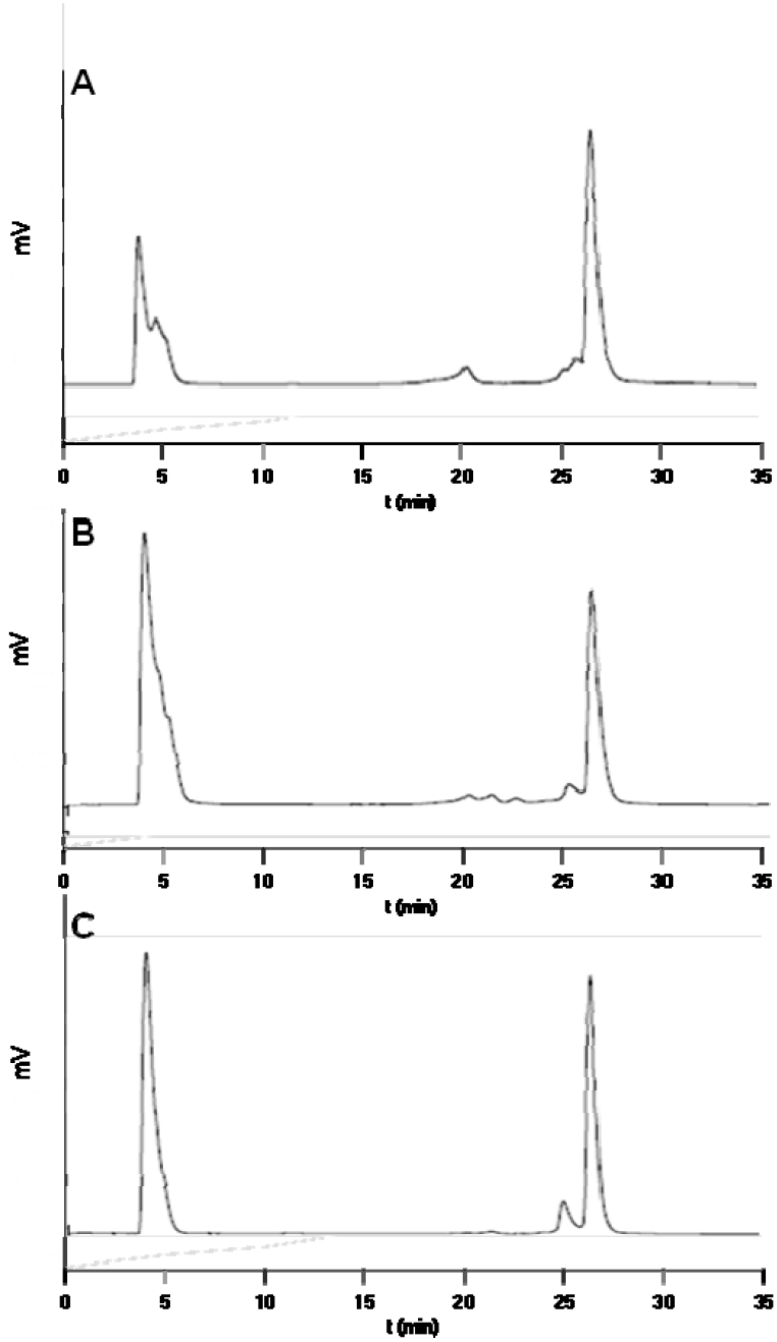

Figure 3. HPLC radiotraces of the crude reactions from three independent preparations of ^{18}F-labeled 3 eluting at ~26.5 min: A: radiotrace for tumor imaging, B: for serum stability assays, and C: for imaging clearance in non-tumor mice. The fraction eluting at ~26 min was collected for further study.

For *in vivo* stability studies, ~100 μCi of 3 in 200 μL PBS was injected into two healthy mice. As expected, the tracer cleared rapidly from the lungs to the liver, intestine, pancreas, and predominantly the bladder (see supporting information for images and time activity curves). In order to investigate tumor-specific uptake, eight mice, of which four were pre-blocked with 100 μg BBN, were injected with 10-20 μCi of 3 and after 60 minutes were sacrificed to generate *ex vivo* biodistribution data that showed in the unblocked specific tumor uptake of 1.27 ± 0.35 %ID/g and a tumor:blood ratio of ~1.5 mice while in the blocked mice, tumor uptake of 0.88 ± 0.26 %ID/g (P-value = 0.009) and a tumor:blood ratio of ~0.9. These data are summarized in **Figure 5**. As expected, blocking also reduced uptake in the pancreas. To corroborate these data, ^{18}F-labeled 3 was prepared at higher specific activity (Radiosynthesis 2) and injected into two mice which presented two separate human prostate cancer xenograft tumors (PC3), of which one had been pre-blocked via tail vein injection with 100 μg BBN, were injected with 100 μCi of 3. Mice were imaged by dynamic PET-CT for 90 minutes. Specific tumor uptake was observed in both tumors with maximal uptake observed approximately 60 minutes post injection. The pre-blocked mouse showed much less tumor uptake (**Figure 6**). Taken together, these *in vivo* images and biodistribution data demonstrate GRPR-specific tumor uptake of 3.

Discussion

Herein, we have radiosyntheisized an alkyne-^{18}F-ArBF_3^- under aqueous conditions that is cleanly conjugated to a bombesin antagonist in a one-pot-two-step procedure, providing func-

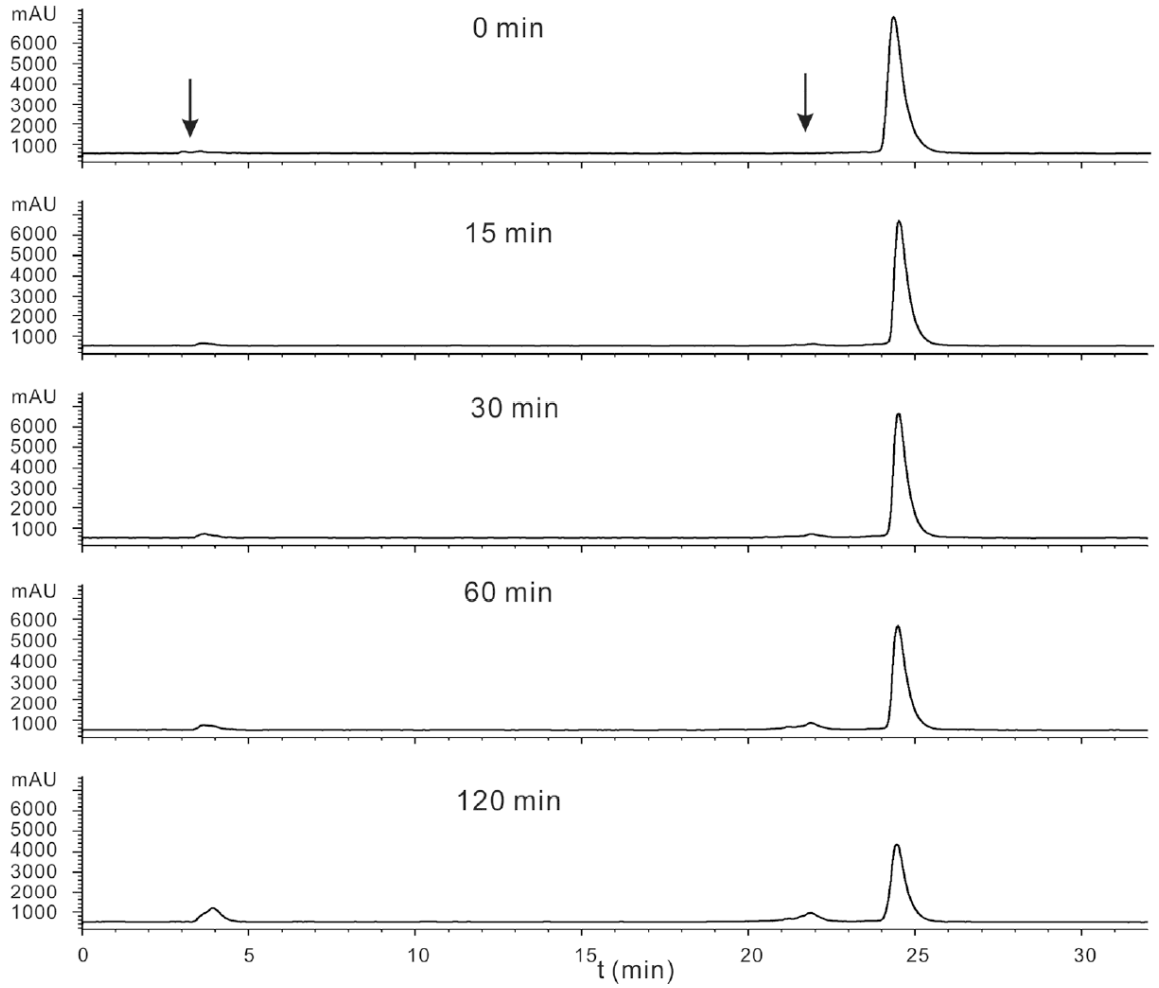

Figure 4. Purified BBN-^{18}F-ArBF$_3^-$ was diluted in saline buffer (2 mL). For each assay, the saline solution (200 μL) was mixed with plasma (200 μL), incubated at 30°C for 0, 15, 30, 60 and 120, and quenched by the addition of 75% aqueous CH_3CN (400 μL). Following centrifugation, the supernatant was isolated, filtered, and analyzed by HPLC for further analysis. The red arrows indicate peaks that represent time dependent degradation products and free ^{18}F-fluoride ion or other high polar material.

tional images of GRPR-positive tumors. Notably, this method uses nanomole (microgram) quantities of precursor borimidine and azidopeptide while high specific activity >1 Ci/μmol was achieved using just 30 mCi of ^{18}F-activity. The use of relatively low levels of radioactive material provides reasonable yields of radiotracer at high specific activities while minimizing safety concerns. Nevertheless, use of 800 mCi of ^{18}F-activity as commonly used in production labs, will provide considerably higher specific activities as well as higher yields, a proposition that we have belabored elsewhere at length [3, 56].

While we expect that specific activities can be increased if needed, the values herein are on par with those previously reported for ^{64}Cu-labeled BBN derivatives [57] leading to the conclusion that the somewhat inferior image quality herein can be a complex manifestation that is only partially ensured by appropriately high specific activity and may be highly sensitive to several factors including prosthetic hydrophobicity and/or radiotracer clearance. An example of such complications is seen with the very hydrophobic ^{18}F-SiFA-BBN-derivative that was labeled at a specific activity in excess of 6 Ci/μmol, yet tumor uptake was lower than in blood suggesting that tracer lipophilicity could adversely impede imaging and result in blood-pool retention [42]. A notable advantage of ^{18}F-ArBF$_3^-$ prosthetics is that they are inherently polar, non-coordinating anions and there-

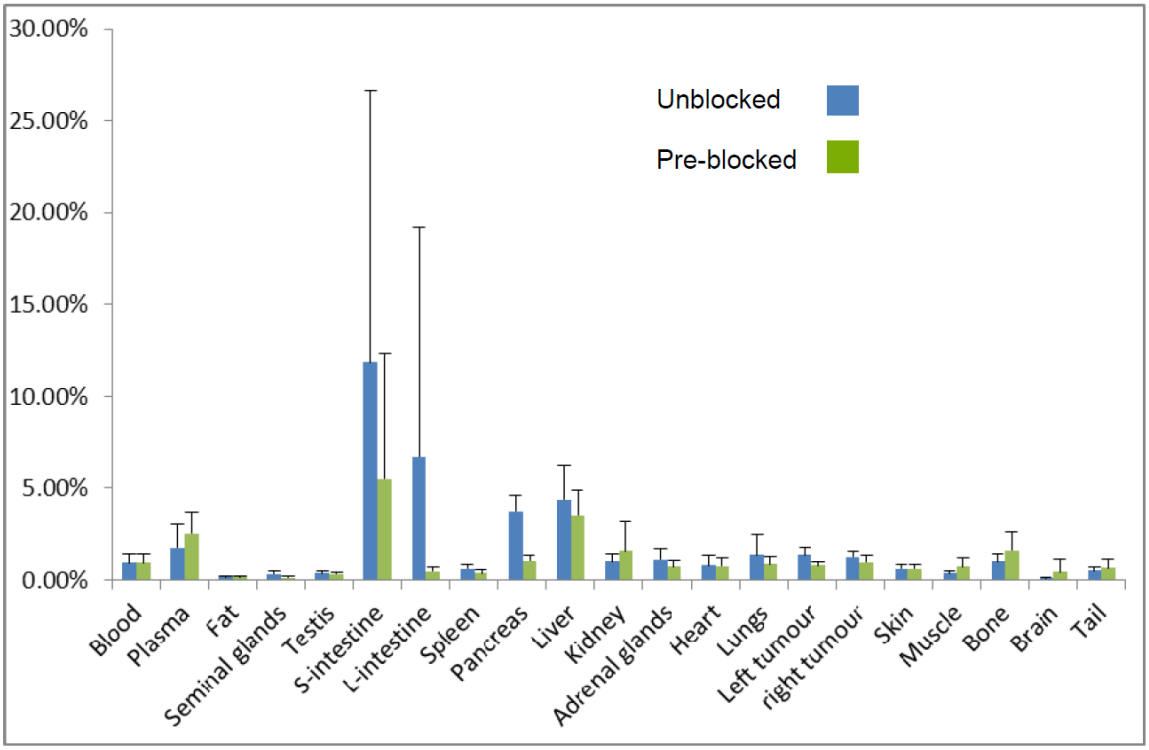

Figure 5. *Ex-vivo* Biodistribution data; blue bars show the average %ID/g from the unblocked animals (n=4) while green bars show the average %ID/g from blocked animals (n=4).

fore expedite blood clearance. More detailed work will be needed to examine the effect of specific activity on image quality in the context of this and other bombesin agonists and antagonists.

In terms of image quality, the %ID/g and tumor-to-muscle and tumor-to-blood ratios were somewhat lower than desired. This is in stark contrast to other BBN analogs labeled with ^{68}Ga and ^{64}Cu that provided extraordinarily high contrast images [25]. While more work will be needed to verify the cause of these lower uptake values, it is likely that imaging with *this* particular antagonist gives lower quality images irrespective of what means are used for radiolabeling. Nevertheless, side-by-side comparisons of this and other antagonists, where each is labeled with the ^{18}F-ArBF$_3^-$, as well as comparison of images obtained when this antagonist is labeled with different labeling modalities, will provide a more definitive assessment as to the cause of low apparent tumor uptake herein. Finally, clearance is very rapid with >50% ID/g clearing to the bladder (data not shown). This along with moderate serum stability would also account for lower tumor uptake. Typically, the development of a clinically used tracer will require various chemical modifications to the peptide and/or the linker to modulate tumor clearance and/or increase affinity.

In these images, bone uptake (0.67 – 1.2 %ID/g) was also observed. Although this may be of some concern, this value is low and is consistent with what has been previously observed with ^{64}Cu- labeled BBN analogs [33, 34] as well as with ^{18}F-SiFA-labeled BBN that also exhibited solvolytic fluoride ion loss [42, 58]. Herein, apparent bone uptake might be due to a) trace amounts of free ^{18}F-fluoride ion i.e. 1% that were not removed, b) specific bone uptake of BBN-^{18}F-ArBF$_3^-$ or its metabolites and c) solvolytic/metabolic defluoridation of the ^{18}F-ArBF$_3^-$. Notably previous reports on the *in vivo* imaging of tracers linked to the *same* ^{18}F-ArBF$_3^-$ did not reveal bone uptake, which would suggest that solvolytic defluoridation may not be the cause of bone revelation here. Serum stability assays however showed a new radiolabeled product eluting at 22 min to sug-

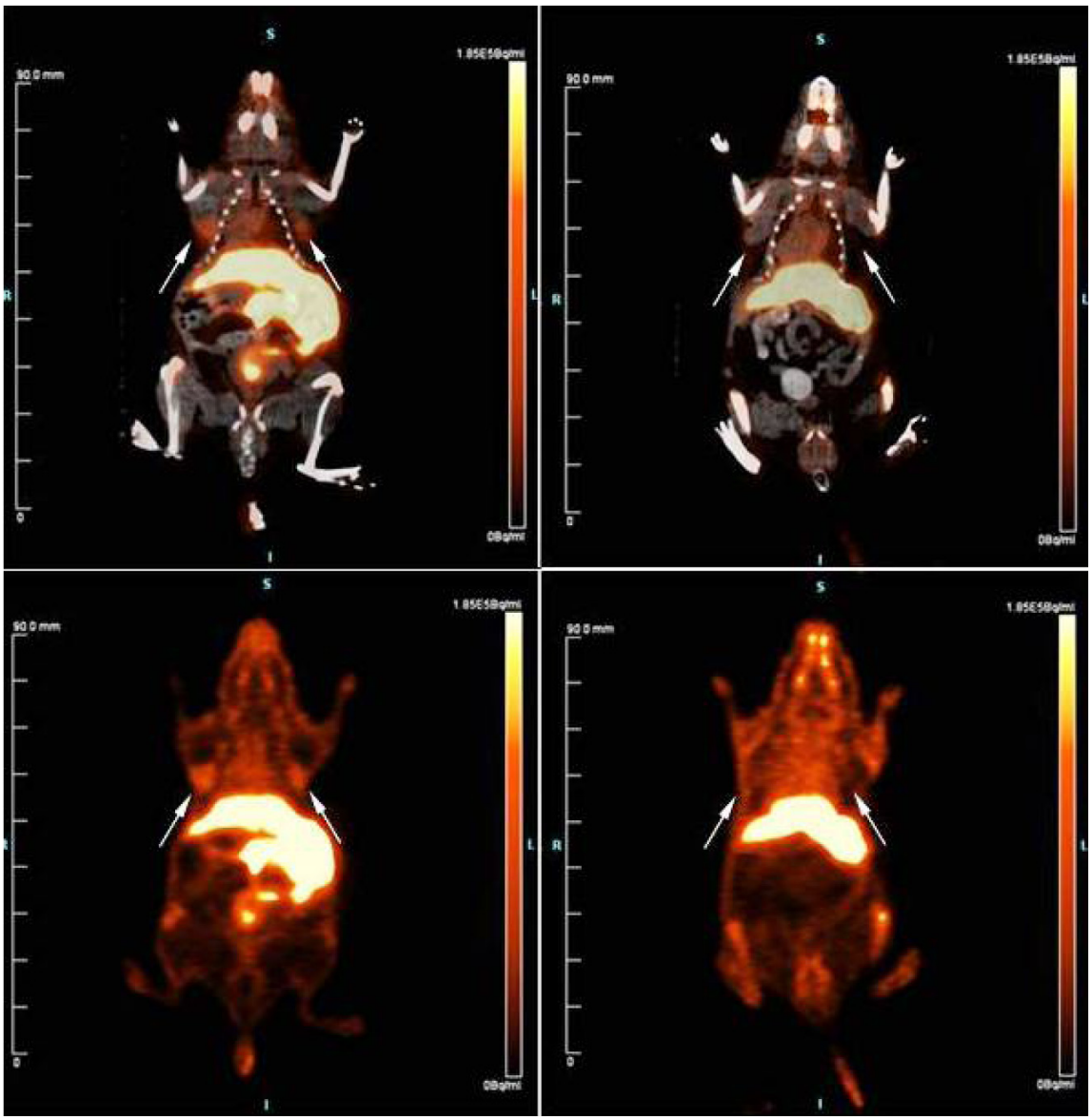

Figure 6. PET-CT and PET images at 60 minutes: top panels are a combined PET-CT while bottom panels are the pure PET image; unblocked mouse is shown in the left while the blocked mouse (pre-injected with 100 μg BBN(6-14)) is shown on the right; white arrows indicate position of xenograft tumors that have been derived from PC3 human prostate adenocarcinoma cells.

gest proteolytic degradation while a very polar species which eluted at 4 min is consistent with fluoride liberation. In terms of fluoride solvolysis, the $ArBF_3^-$ is known to solvolyze slowly, (k_{obs} ~ 0.3±.2 · 10^{-3} min^{-1}, as measured by ^{19}F-NMR spectroscopy) however given this rate constant, the release of 10% fluoride would likely take four hours, not two. Nevertheless, inasmuch as bone signal will need to be further minimized, use of other ^{18}F-labeled $ArBF_3^-$ conjugates known to defluoridate even more slowly than the one used herein [59, 60] will shed light on whether bone uptake arises from solvolytic/metabolic defluoridation of the ^{18}F-$ArBF_3^-$ or accumulation of the ^{18}F-$ArBF_3^-$-BBN conjugate itself.

Conclusion

The use of boron to capture ^{18}F-fluoride ion represents a relatively new labeling platform that provides a distinct advantage of working in

aqueous conditions and mild temperatures to rapidly afford a highly polar, rapidly clearing ^{18}F-ArBF$_3^-$ anion that enhances the clearance of ligands to which it is attached. Here we have extended a rapid one-pot-two-step method that uses low amounts of ^{18}F-activity and only microgram quantities of precursors to labeling bombesin, which revealed tumor-specific uptake. As rapid labeling times are essential for working with a short-lived isotope such as ^{18}F-fluorine, this work represents an attractive means of labeling peptides with a uniquely polar radiosython, in what represents one of the more rapid one-pot-two-step labeling methods reported to date. In summary the salient advantages embodied in this labeling method are: i) use of low levels of radioactivity (< 50 mCi), ii) rapid synthesis time: ~40 minutes with reasonable overall isolated radiochemical yields, iii) the use of aqueous conditions at room temperature, iv) the production of a highly polar, rapidly clearing ^{18}F-labeled *anion*, v) a one pot reaction that does not require workup between steps, and vi) a Cu^+-catalyzed [2+3] cycloaddition which, based on the well-known generality of click chemistry should be extendable to any peptide, oligonucleotide, and antibody worthy of labeling.

Acknowledgements

This work was supported by a grant from the Canadian Cancer Society #20071.

Address correspondence to: Dr. David M Perrin, Chemistry Department, UBC, 2036 Main Mall, Vancouver, B.C., V6T-1Z1, Canada. Phone: 604 8220567; E-mail: dperrin@chem.ubc.ca

References

[1] Okarvi SM. Recent progress in fluorine-18 labelled peptide radiopharmaceuticals. Eur J Nucl Med 2001; 28: 929-938.

[2] Ting R, Harwig C, Lo J, Li Y, Adam MJ, Ruth TJ and Perrin DM. Substituent Effects on Aryltrifluoroborate Solvolysis in Water: Implications for Suzuki-Miyaura Coupling and the Design of Stable ^{18}F-Labeled Aryltrifluoroborates for Use in PET Imaging. J Org Chem 2008; 73: 4662-4670.

[3] Ting R, Harwig CW, auf dem Keller U, McCormick S, Austin P, Overall CM, Adam MJ, Ruth TJ and Perrin DM. Towards [^{18}F]-Labeled Aryltrifluoroborate Radiotracers - In Vivo PET Imaging of Stable Aryltrifluoroborate Clearance in Mice. J Am Chem Soc 2008; 130: 12045-12055.

[4] Ting R, Lo J, Adam MJ, Ruth TJ and Perrin DM. Capturing aqueous (18)F -fluoride with an arylboronic ester for PET: Synthesis and aqueous stability of a fluorescent (18)F -labeled aryltrifluoroborate. J Fluor Chem 2008; 129: 349-358.

[5] Keller UAD, Bellac CL, Li Y, Lou YM, Lange PF, Ting R, Harwig C, Kappelhoff R, Dedhar S, Adam MJ, Ruth TJ, Benard F, Perrin DM and Overall CM. Novel Matrix Metalloproteinase Inhibitor F-18 Marimastat-Aryltrifluoroborate as a Probe for In vivo Positron Emission Tomography Imaging in Cancer. Cancer Res 2010; 70: 7562-7569.

[6] Abiraj K, Mansi R, Tamma ML, Fani M, Forrer F, Nicolas G, Cescato R, Reubi JC and Maecke HR. Bombesin Antagonist-Based Radioligands for Translational Nuclear Imaging of Gastrin-Releasing Peptide Receptor-Positive Tumors. J Nucl Med 2011; 52: 1970-1978.

[7] Ambrosini V, Tomassetti P, Franchi R and Fanti S. Imaging of NETs with PET radiopharmaceuticals. Quar J Nucl Med and Mol Imag 2010; 54: 16-23.

[8] Aigner A. Applications of RNA interference: current state and prospects for siRNA-based strategies in vivo. App Microbiol and Biotech 2007; 76: 9-21.

[9] Moses JE and Moorhouse AD. The growing applications of click chemistry. Chem Soc Rev 2007; 36: 1249-1262.

[10] Glaser M and Arstad E. "Click labeling" with 2-F-18 fluoroethylazide for positron emission tomography. Bioconjug Chem 2007; 18: 989-993.

[11] Thonon D, Kech C, Paris J, Lemaire C and Luxen A. New Strategy for the Preparation of Clickable Peptides and Labeling with 1-(Azidomethyl)-4- F-18 -fluorobenzene for PET. Bioconjug Chem 2009; 20: 817-823.

[12] Mercier F, Paris J, Kaisin G, Thonon D, Flagothier J, Teller N, Lemaire C and Luxen A. General Method for Labeling siRNA by Click Chemistry with Fluorine-18 for the Purpose of PET Imaging. Bioconjug Chem 2011; 22: 108-114.

[13] Kostikov AP, Iovkova L, Chin J, Schirrmacher E, Wangler B, Wangler C, Jurkschat K, Cosa G and Schirrmacher R. N-(4-(di-tert-butyl F-18 fluorosilyl)benzyl)-2-hydroxy-N, N-dimethylethylammonium bromide (F-18 SiFAN(+)Br(-)): A novel lead compound for the development of hydrophilic SiFA-based prosthetic groups for F-18-labeling. J Fluor Chem 2011; 132: 27-34.

[14] Carpenter RD, Hausner SH and Sutcliffe JL. Copper-Free Click for PET: Rapid 1,3-Dipolar Cycloadditions with a Fluorine-18 Cyclooctyne. Acs Med Chem Lett 2011; 2: 885-889.

[15] Priem T, Bouteiller C, Camporese D, Romieu A and Renard PY. Synthesis and reactivity of a

bis-sultone cross-linker for peptide conjugation and F-18 -radiolabelling via unusual "double click" approach. Org Biomol Chem 2012; 10: 1068-1078.

[16] Olberg DE, Cuthbertson A, Solbakken M, Arukwe JM, Qu H, Kristian A, Bruheim S and Hjelstuen OK. Radiosynthesis and Biodistribution of a Prosthetic Group ((18)F-FENMA) Conjugated to Cyclic RGD Peptides. Bioconjug Chem 2010; 21: 2297-2304.

[17] Jeon J, Shen B, Xiong L, Miao Z, Lee KH, Rao J and Chin FT. Efficient Method for Site-Specific ^{18}F-Labeling of Biomolecules Using the Rapid Condensation Reaction between 2-Cyanobenzothiazole and Cysteine. Bioconjug Chem 2012; 23: 1902–1908.

[18] Honer M, Mu LJ, Stellfeld T, Graham K, Martic M, Fischer CR, Lehmann L, Schubiger PA, Ametamey SM, Dinkelborg L, Srinivasan A and Borkowski S. F-18-Labeled Bombesin Analog for Specific and Effective Targeting of Prostate Tumors Expressing Gastrin-Releasing Peptide Receptors. J Nucl Med 2011; 52: 270-278.

[19] Butters M, Harvey JN, Jover J, Lennox AJJ, Lloyd-Jones GC and Murray PM. Aryl Trifluoroborates in Suzuki-Miyaura Coupling: The Roles of Endogenous Aryl Boronic Acid and Fluoride. Angew Chem Int Ed 2010; 49: 5156-5160.

[20] Markwalder R and Reubi JC. Gastrin-releasing peptide receptors in the human prostate: Relation to neoplastic transformation. Cancer Res 1999; 59: 1152-1159.

[21] Halmos G, Wittliff JL and Schally AV. Characterization of bombesin/gastrin-releasing peptide receptors in human breast cancer and their relationship to steroid receptor expression. Cancer Res 1995; 55: 280-287.

[22] ToiScott M, Jones CLA and Kane MA. Clinical correlates of bombesin-like peptide receptor subtype expression in human lung cancer cells. Lung Cancer 1996; 15: 341-354.

[23] Kaltsas GA, Besser GM and Grossman AB. The diagnosis and medical management of advanced neuroendocrine tumors. Endocrine Rev 2004; 25: 458-511.

[24] Cuttitta F, Carney DN, Mulshine J, Moody TW, Fedorko J, Fischler A and Minna JD. Bombesin-like peptides can function as autocrine growth factors in human small-cell lung cancer. Nature 1985; 316: 823-826.

[25] Cornelio DB, Roesler R and Schwartsmann G. Gastrin-releasing peptide receptor as a molecular target in experimental anticancer therapy. Ann Oncol 2007; 18: 1457-1466.

[26] Banerjee SR, Pullambhatla M, Byun Y, Nimmagadda S, Green G, Fox JJ, Horti A, Mease RC and Pomper MG. 68Ga-Labeled Inhibitors of Prostate-Specific Membrane Antigen (PSMA) for Imaging Prostate Cancer. J Med Chem 2010; 53: 5333–5341.

[27] Mansi R, Wang XJ, Forrer F, Waser B, Cescato R, Graham K, Borkowski S, Reubi JC and Maecke HR. Development of a potent DOTA-conjugated bombesin antagonist for targeting GRPr-positive tumours. Eur J Nucl Med and Mol Imag 2011; 38: 97-107.

[28] Min K, Jo H, Song K, Cho M, Chun YS, Jon S, Kim WJ and Ban C. Dual-aptamer-based delivery vehicle of doxorubicin to both PSMA (+) and PSMA (-) prostate cancers. Biomaterials 2011; 32: 2124-2132.

[29] Baidoo KE, Lin KS, Zhan YG, Finley P, Scheffel U and Wagner HN. Design, synthesis, and initial evaluation of high-affinity technetium bombesin analogues. Bioconjug Chem 1998; 9: 218-225.

[30] Smith CJ, Volkert WA and Hoffman TJ. Radiolabeled peptide conjugates for targeting of the bombesin receptor superfamily subtypes. Nucl Med Biol 2005; 32: 733-740.

[31] Kunstler JU, Veerendra B, Figueroa SD, Sieckman GL, Rold TL, Hoffman TJ, Smith CJ and Pietzsch HJ. Organometallic Tc-99m(III) '4+1' bombesin(7-14) conjugates: Synthesis, radiolabeling, and in vitro/in vivo studies. Bioconjug Chem 2007; 18: 1651-1661.

[32] Zeglis BM and Lewis JS. A practical guide to the construction of radiometallated bioconjugates for positron emission tomography. Dalt Trans 2011; 40: 6168-6195.

[33] Rogers BE, Bigott HM, McCarthy DW, Della Manna D, Kim J, Sharp TL and Welch MJ. MicroPET imaging of a gastrin-releasing peptide receptor-positive tumor in a mouse model of human prostate cancer using a Cu-64-labeled bombesin analogue. Bioconjug Chem 2003; 14: 756-763.

[34] Garrison JC, Rold TL, Sieckman GL, Figueroa SD, Volkert WA, Jurisson SS and Hoffman TJ. In vivo evaluation and small-animal PET/CT of a prostate cancer mouse model using Cu-64 bombesin analogs: Side-by-side comparison of the CB-TE2A and DOTA chelation systems. J Nucl Med 2007; 48: 1327-1337.

[35] Parry JJ, Andrews R and Rogers BE. MicroPET imaging of breast cancer using radiolabeled bombesin analogs targeting the gastrin-releasing peptide receptor. Breast Cancer Res and Treatment 2007; 101: 175-183.

[36] Hoffman TJ and Smith CJ. True radiotracers: Cu-64 targeting vectors based upon bombesin peptide. Nucl Med Biol 2009; 36: 579-585.

[37] Dimitrakopoulou-Strauss A, Hohenberger P, Haberkorn U, Macke HR, Eisenhut M and Strauss LG. Ga-68-Labeled bombesin studies in patients with gastrointestinal stromal tu-

mors: Comparison with F-18-FDG. J Nucl Med 2007; 48: 1245-1250.

[38] Dimitrakopoulou-Strauss A, Seiz M, Tuettenberg J, Schmieder K, Eisenhut M, Haberkorn U and Strauss LG. Pharmacokinetic Studies of Ga-68-Labeled Bombesin (Ga-68-BZH(3)) and F-18 FDG PET in Patients With Recurrent Gliomas and Comparison to Grading Preliminary Results. Clin Nucl Med 2011; 36: 101-108.

[39] Pandya DN, Dale AV, Kim JY, Lee H, Ha YS, An GI and Yoo J. New Macrobicyclic Chelator for the Development of Ultrastable Cu-64-Radiolabeled Bioconjugate. Bioconjug Chem 2012; 23: 330-335.

[40] Ait-Mohand S, Fournier P, Dumulon-Perreault V, Kiefer GE, Jurek P, Ferreira CL, Benard F and Guerin B. Evaluation of Cu-64-Labeled Bifunctional Chelate-Bombesin Conjugates. Bioconjug Chem 2011; 22: 1729-1735.

[41] Zhang XZ, Cai WB, Cao F, Schreibmann E, Wu Y, Wu JC, Xing L and Chen XY. F-18-labeled bombesin analogs for targeting GRP receptor-expressing prostate cancer. J Nucl Med 2006; 47: 492-501.

[42] Hoehne A, Mu L, Honer M, Schubiger PA, Ametamey SM, Graham K, Stellfeld T, Borkowski S, Berndorff D, Klar U, Voigtmann U, Cyr JE, Friebe M, Dinkelborg L and Srinivasan A. Synthesis, F-18-labeling, and in vitro and in vivo studies of bombesin peptides modified with silicon-based building blocks. Bioconjug Chem 2008; 19: 1871-1879.

[43] Campbell-Verduyn LS, Mirfeizi L, Schoonen AK, Dierckx RA, Elsinga PH and Feringa BL. Strain-Promoted Copper-Free "Click" Chemistry for ^{18}F Radiolabeling of Bombesin. Angew Chem Int Ed 2011; 50: 11117-11120.

[44] Schirrmacher E, Wangler B, Cypryk M, Bradtmoller G, Schafer M, Eisenhut M, Jurkschat K and Schirrmacher R. Synthesis of p-(Di-tert-butyl (18)F fluorosilyl)benzaldehyde (F-18 SiFA-A) with high specific activity by isotopic exchange: A convenient Labeling synthon for the F-18-labeling of n-amino-oxy derivatized peptides. Bioconjug Chem 2007; 18: 2085-2089.

[45] Schirrmacher R, Bradtmoller G, Schirrmacher E, Thews O, Tillmanns J, Siessmeier T, Buchholz HG, Bartenstein P, Waengler B, Niemeyer CM and Jurkschat K. F-18-labeling of peptides by means of an organosilicon-based fluoride acceptor. Angew Chem Int Ed 2006; 45: 6047-6050.

[46] Kostikov AP, Chin J, Orchowski K, Niedermoser S, Kovacevic MM, Aliaga A, Jurkschat K, Wangler B, Wangler C, Wester HJ and Schirrmacher R. Oxalic Acid Supported Si-F-18-Radiofluorination: One-Step Radiosynthesis of N-Succinimidyl 3-(Di-tert-butyl F-18 fluorosilyl) benzoate (F-18 SiFB) for Protein Labeling. Bioconjug Chem 2012; 23: 106-114.

[47] Cescato R, Maina T, Nock B, Nikolopoulou A, Charalambidis D, Piccand V and Reubi JC. Bombesin receptor antagonists may be preferable to agonists for tumor targeting. J Nucl Med 2008; 49: 318-326.

[48] Nanda PK, Pandey U, Bottenus BN, Rold TL, Sieckman GL, Szczodroski AF, Hoffman TJ and Smith CJ. Bombesin analogues for gastrin-releasing peptide receptor imaging. Nucl Med Biol 2012; 39: 461-471.

[49] Iwadate N and Suginome M. Synthesis of masked haloareneboronic acids via iridium-catalyzed aromatic C-H borylation with 1,8-naphthalenediaminatoborane (danBH). Journal of Organomet Chem 2009; 694: 1713-1717.

[50] Noguchi H, Shioda T, Chou CM and Suginome M. Differentially protected, benzenediboronic acids: Divalent cross-coupling modules for the efficient synthesis of boron-substituted oligoarenes. Org Lett 2008; 10: 377-380.

[51] Nock B, Nikolopoulou A, Chiotellis E, Loudos G, Maintas D, Reubi JC and Maina T. Tc-99m Demobesin 1, a novel potent bombesin analogue for GRP receptor-targeted tumour imaging. Eur J Nucl Med and Mol Imag 2003; 30: 247-258.

[52] Vedejs E, Chapman RW, Fields SC, Lin S and Schrimpf MR. Conversion of Arylboronic Acids into Potassium Aryltrifluoroborates - Convenient Precursors of Arylboron Difluoride Lewis-Acids. J Org Chem 1995; 60: 3020-3027.

[53] Quach TD and Batey RA. Ligand- and base-free copper(II)-catalyzed C-N bond formation: Cross-coupling reactions of organoboron compounds with aliphatic amines and anilines. Org Lett 2003; 5: 4397-4400.

[54] Molander GA and Ham J. Synthesis of functionalized organotrifluoroborates via the 1,3-dipolar cycloaddition of azides. Org Lett 2006; 8: 2767-2770.

[55] Zhang HW, Chen JH, Waldherr C, Hinni K, Waser B, Reubi JC and Maecke HR. Synthesis and evaluation of bombesin derivatives on the basis of pan-bombesin peptides labeled with indium-111, lutetium-177, and yttrium-90 for targeting bombesin receptor-expressing tumors. Cancer Res 2004; 64: 6707-6715.

[56] Li Y, Ting R, Harwig CW, Keller UAD, Bellac CL, Lange PF, Inkster JAH, Schaffer P, Adam MJ, Ruth TJ, Overall CM and Perrin DM. Towards kit-like F-18-labeling of marimastat, a noncovalent inhibitor drug for in vivo PET imaging cancer associated matrix metalloproteases. Medchemcomm 2011; 2: 942-949.

[57] Lears KA, Ferdani R, Liang KX, Zheleznyak A, Andrews R, Sherman CD, Achilefu S, Anderson CJ and Rogers BE. In Vitro and In Vivo Evalua-

tion of Cu-64-Labeled SarAr-Bombesin Analogs in Gastrin-Releasing Peptide Receptor-Expressing Prostate Cancer. J Nucl Med 2011; 52: 470-477.

[58] Balentova E, Collet C, Lamande-Langle S, Chretien F, Thonon D, Aerts J, Lemaire C, Luxen A and Chapleur Y. Synthesis and hydrolytic stability of novel 3- F-18 fluoroethoxybis (1-methylethyl)silyl propanamine-based prosthetic groups. J Fluor Chem 2011; 132: 250-257.

[59] Li Y, Asadi A and Perrin DM. Hydrolytic stability of nitrogenous-heteroaryltrifluoroborates under aqueous conditions at near neutral pH. J Fluor Chem 2009; 130: 377-382.

[60] Wade CR, Zhao H and Gabbai FP. Stabilization of zwitterionic aryltrifluoroborates against hydrolysis. Chem Commun 2010; 46: 6380–6381.

Table of Contents

Radiosynthesis of the alkynyl-^{18}F-ArBF_3 and click labeling of N_3-BBN: 3
Radiolabeling for animal imaging 4
Crude radiotrace of the labeling reaction for animal imaging 4
Plasma stability test 5
NMR spectra 10

Synthetic Schemes: Below production of the arylborimidine which is used to give the aryltrifluoroborate and the tetraphenylpinacolate arylboronate which is also converted to the aryltrifluoroborate.

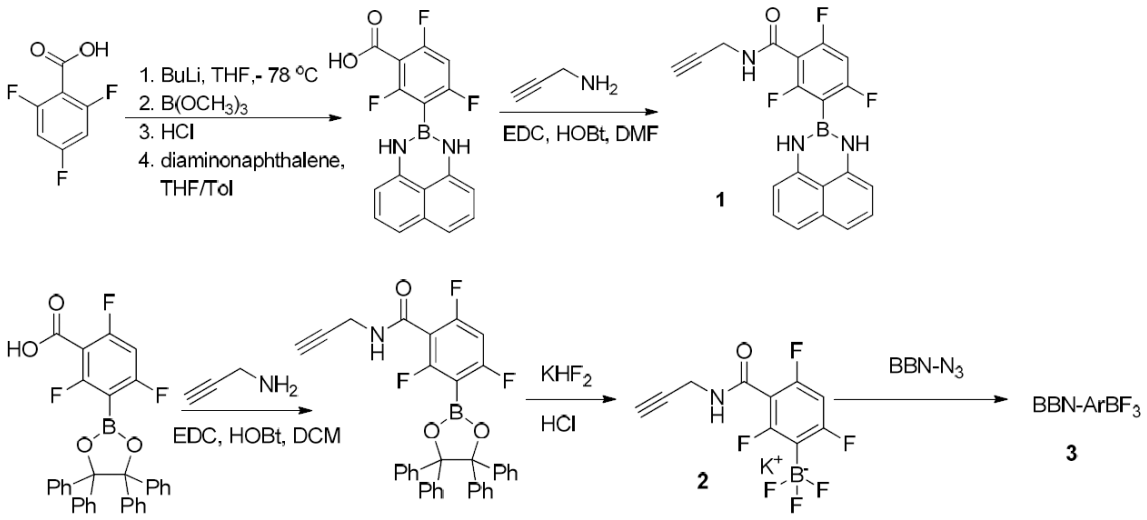

HPLC reinjection of the purified 3 (BBN-ArBF$_3$ after lyophilization) at 229 nm.

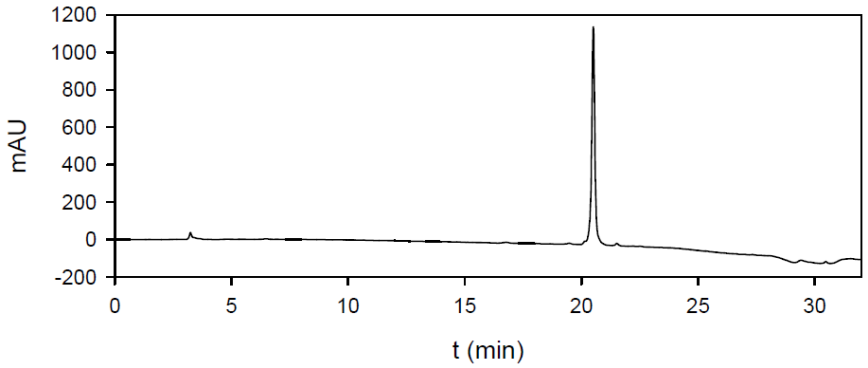

Concentration determination of BBN-ArBF3. An extinction coefficient was calculated to be: 7550 $M^{-1}cm^{-1}$at 280 nm based on values of individual functional groups. Using this value, the concentration of a solution of purified BBN-ArBF$_3$ was determined. This solution was diluted for receptor binding assays by competition with a ^{125}I-labeled variant of bombesin to measure the K_d for the GRP-receptor.

IC50 Assay for BBN-ArBF3.BBN-ArBF$_3$ was stored dry or in 35% aqueous DMSOand was diluted serially for a receptor binding assay using whole cells. The inhibition constant (K_i) of BBN-ArBF$_3$ was determined by performing competitive binding assay using ^{125}I-Tyr-BBN (PerkinElmer) as the radioligand. Briefly, PC-3 human prostate adenocarcinoma cells were cultured in Ham's F-12 and 10% fetal bovine serum and seeded in 6-well plates (1 x 10^5 cells/well). For the binding assay the medium was replaced with RPMI 1640 containing 4.8 mg/mL HEPES, 2 mg/mL BSA and 0.1μM penicillin/streptavidin. The cells were incubated with increasing concentration of BBN-ArBF$_3$peptide ranging from 10 pM to 0.1 μM, in the presence of a constant concentration of 4.2 pmol/L of radioligand in triplicates for 45 min at 37˚C. The cells were rinsed with ice-cold PBS three times and then detached by trypsin and counted in a gamma counter (Cobra-II Auto Gamma, Canberra Packard Canada) to determine the amount of bound radioactivity. Results are shown as counts per minute (CPM) of radioactivity bound to cells vs. log of molar concentration of BBN-ArBF3. Data are presented as mean ± SEM of experiment with each point being performed in triplicate.

The data were analyzed using the GraphPad Prism software.The K_i was calculated to be 3.06 nM.

Radiosynthesis of the alkynyl-^{18}F-ArBF$_3$ and click labeling of N_3-BBN

Following labeling, the reaction was quenched and loaded directly onto the HPLC column. The crude HPLC radiotrace is shown below.

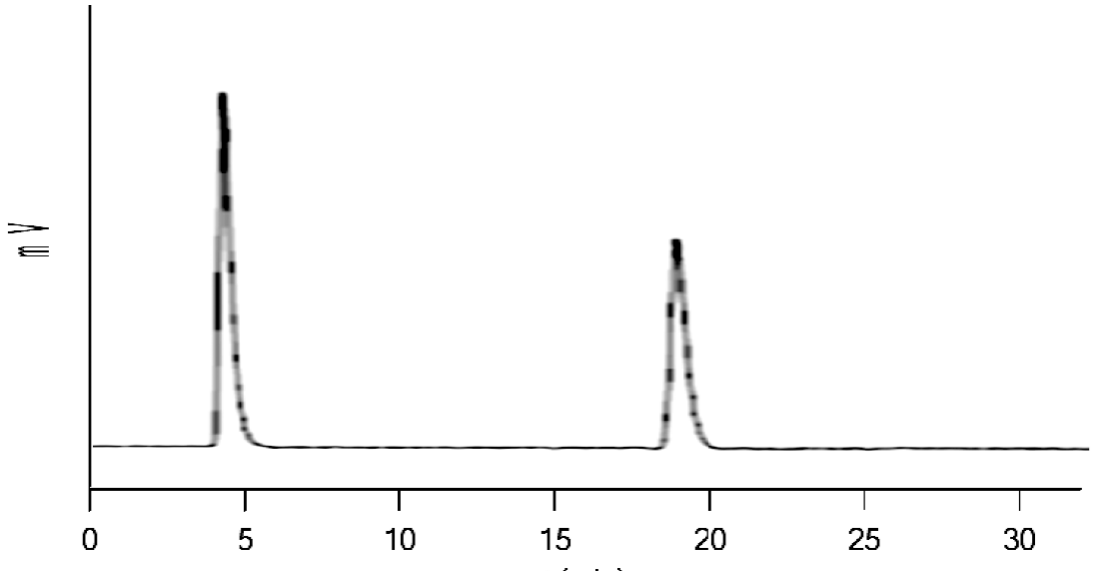

Crude HPLC Radiotrace of the labeled **2**, which eluted at 19 minutes.

Radiolabeling for biodistribution study: The desalted product (2.17 mCi at t= 118 min) was diluted with saline buffer (2 mL) and expedited for biodistribution studies (specific activity calculated to be ~ 0.077 Ci/mmol)

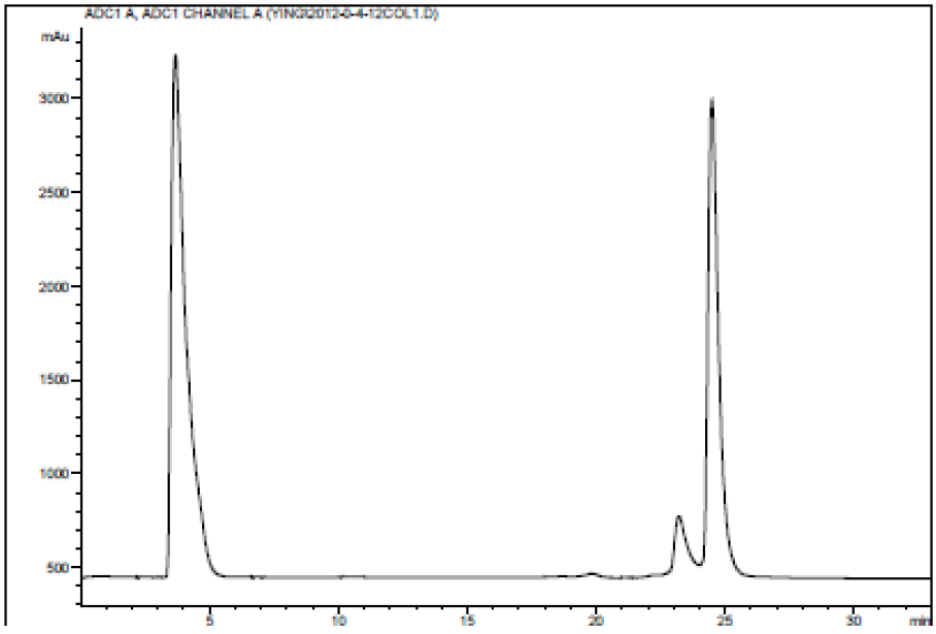

Crude radiotrace of one-pot-two-step radiolabeling: desired conjugate **3** eluted at 25 minutes. A small peak which was less prominent in subsequent labeling reactions was not collected or identified.

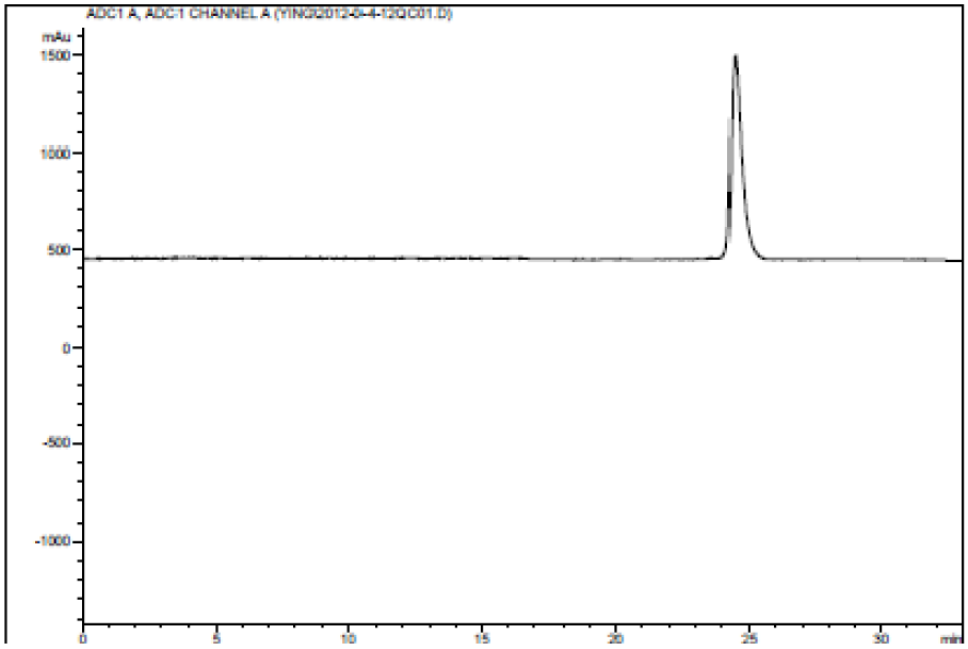

Reinjection to verify the radiochemical purity.

Radiolabeling for animal imaging

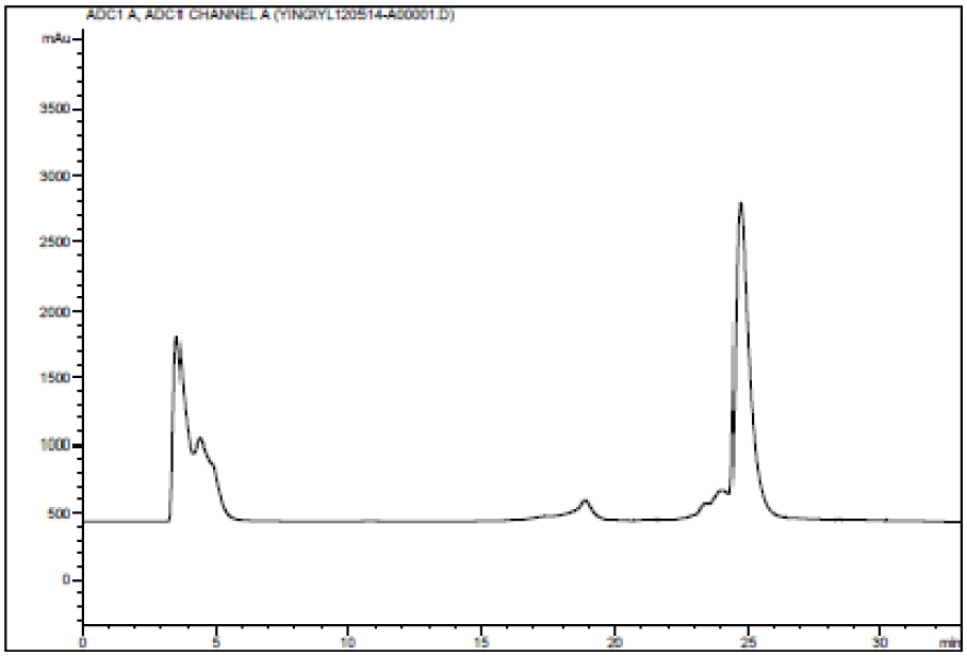

Crude radiotrace of the labeling reaction for animal imaging

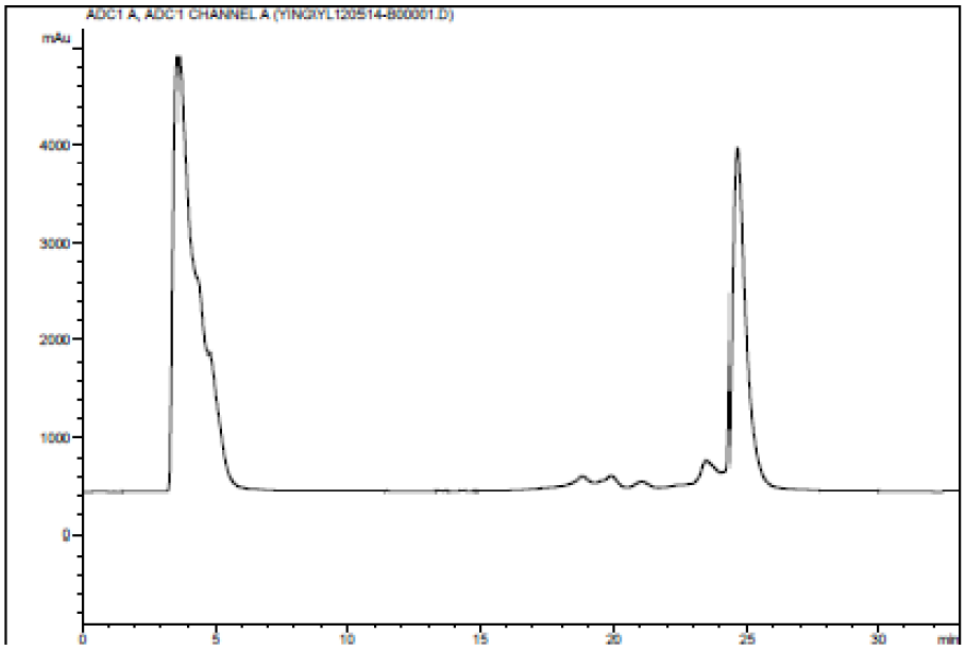

Crude radiotrace of the reaction used for plasma stability assays.

Plasma stability test

BBN-^{18}F-ArBF_3 (4.27 mCi at t= 150 min post EOB) in EtOH (100 mL) was diluted in saline buffer (2 mL). For each assay, the saline solution (200 mL) was mixed with plasma (200 mL), incubated at 30 °C for 0, 15, 30, 60 and 120, and quenched by the addition of 75% aqueous CH_3CN (400 mL). The resulting mixture was then vortexed and centrifuged at 13k rpm for 20 min. The supernatant was isolated, filtered, and analyzed by HPLC for further analysis shown below the percent converted to other products was plotted on the graph below and is similar to serum stabilities seen for bombesin.

Imaging data from healthy mice (5, 30 and 60 min dynamic scans)

Dynamic scan of mice 1&2 from 0-5 min.

Dynamic scan of mice 1&2 from 6-30 min.

Dynamic scan of mice 1&2 from 31-60 min.

Time activity curves for various organs (Liver, Intestine, Heart, Lung, Bone, Kidney, Muscle, Brain, Bladder) :

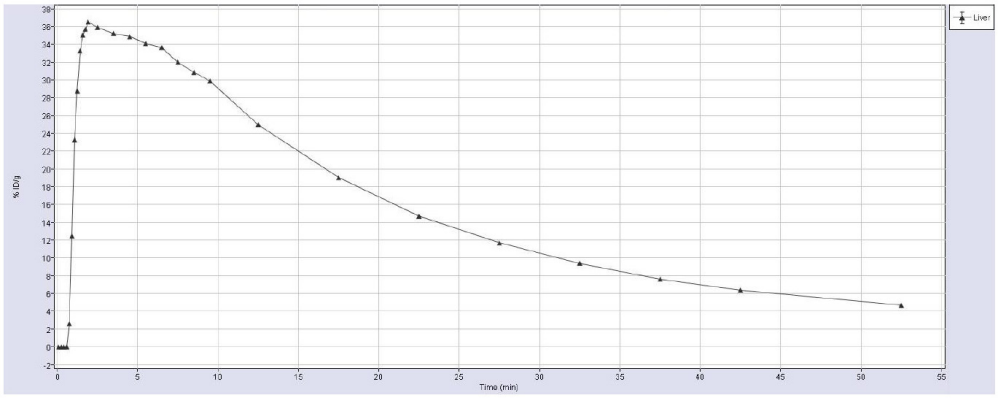

Liver

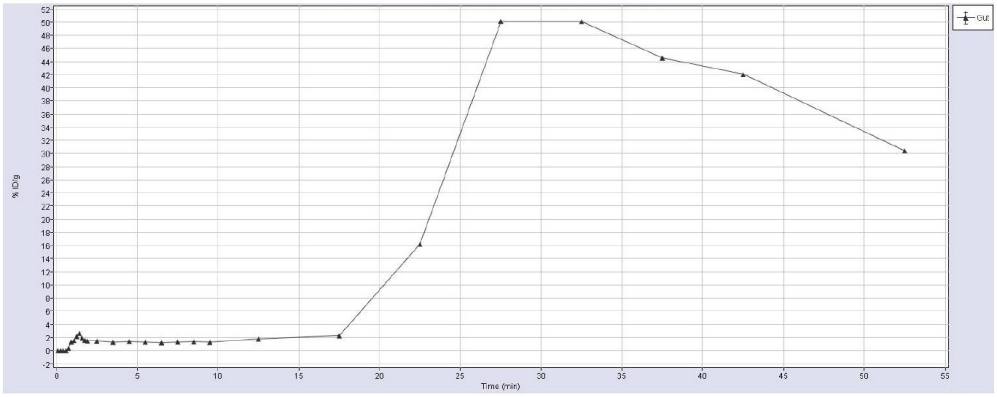

Gut

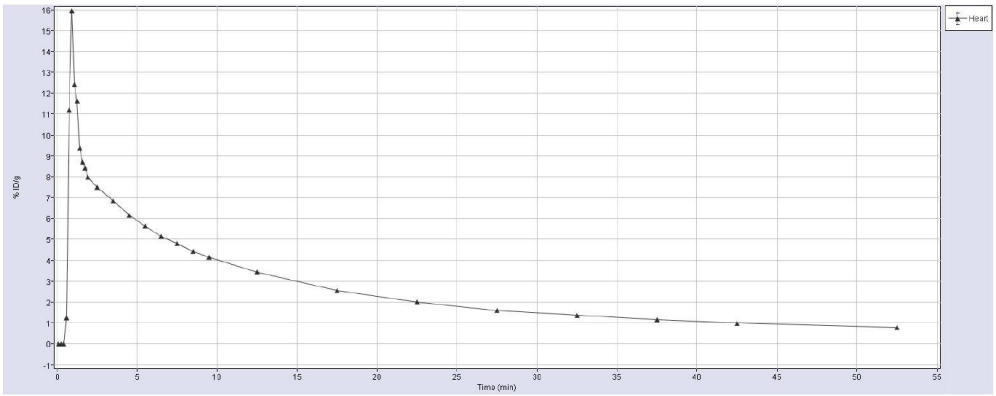

Heart

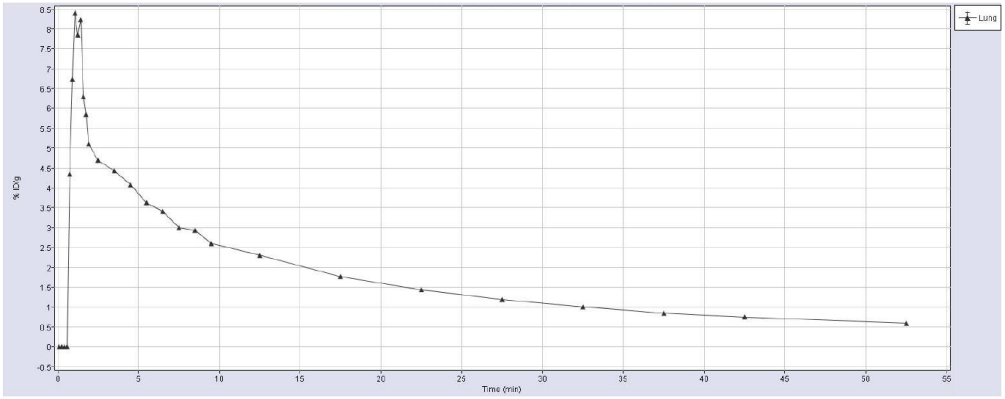

Lung

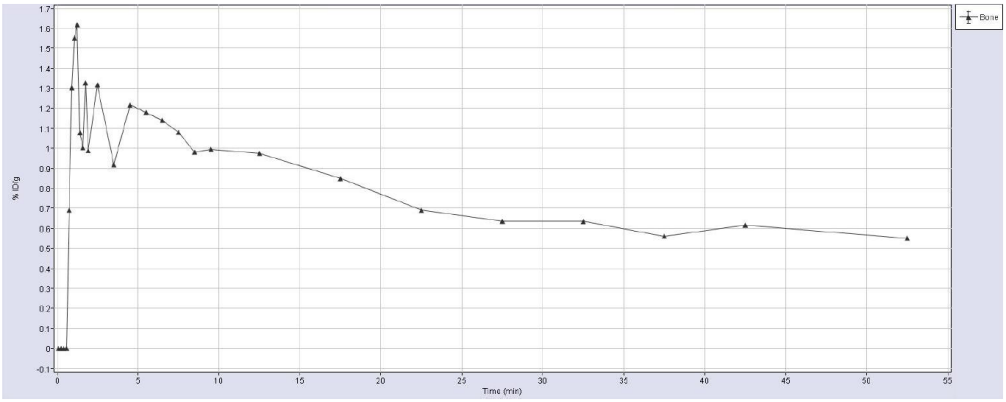

Bone

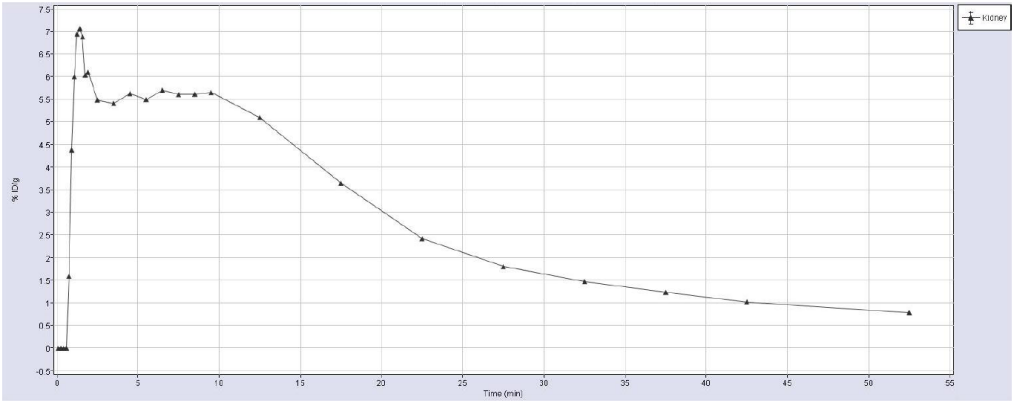

Kidney

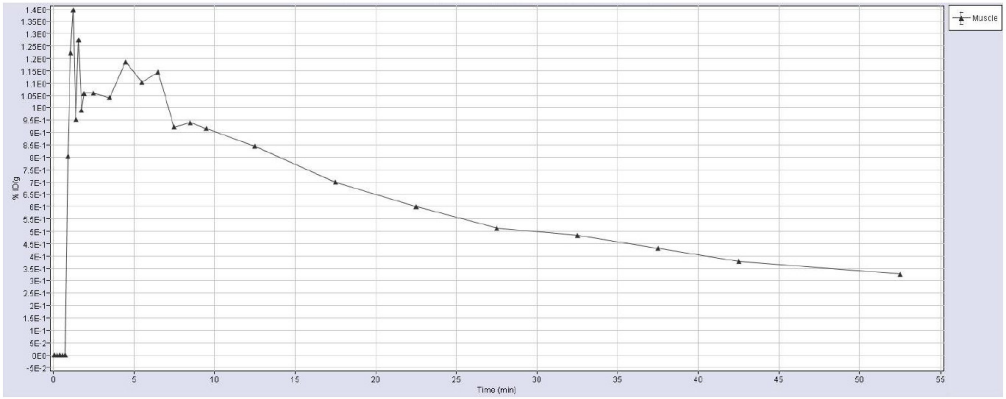

Muscle

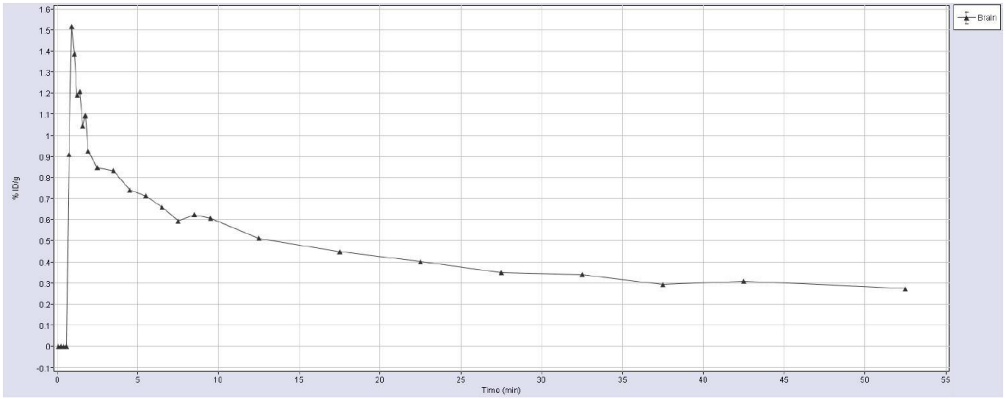

Brain

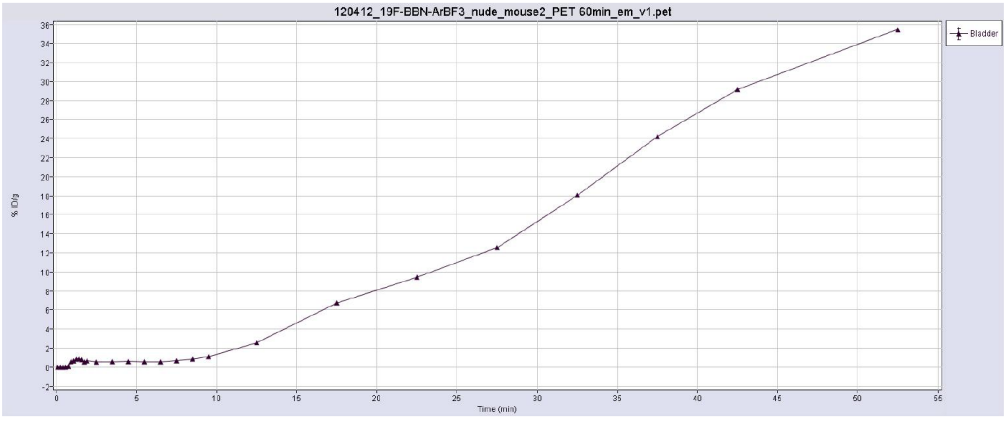

Bladder

Biodistribution of ^{18}F-ArBF$_3$-BBN 60 min post-injection using ROI analysis in healthy mice

Tissue	%ID/g
Heart	0.85 ± 0.09
Lung	0.65 ± 0.07
Liver	4.55 ± 0.21
Intestine*	41.95 ± 10.54
Kidney	0.85 ± 0.08
Bone	0.67 ± 0.19
Muscle	0.30 ± 0.02
Brain	0.33 ± 0.03

* Value for intestine is shown as percentage injected dose (%ID)

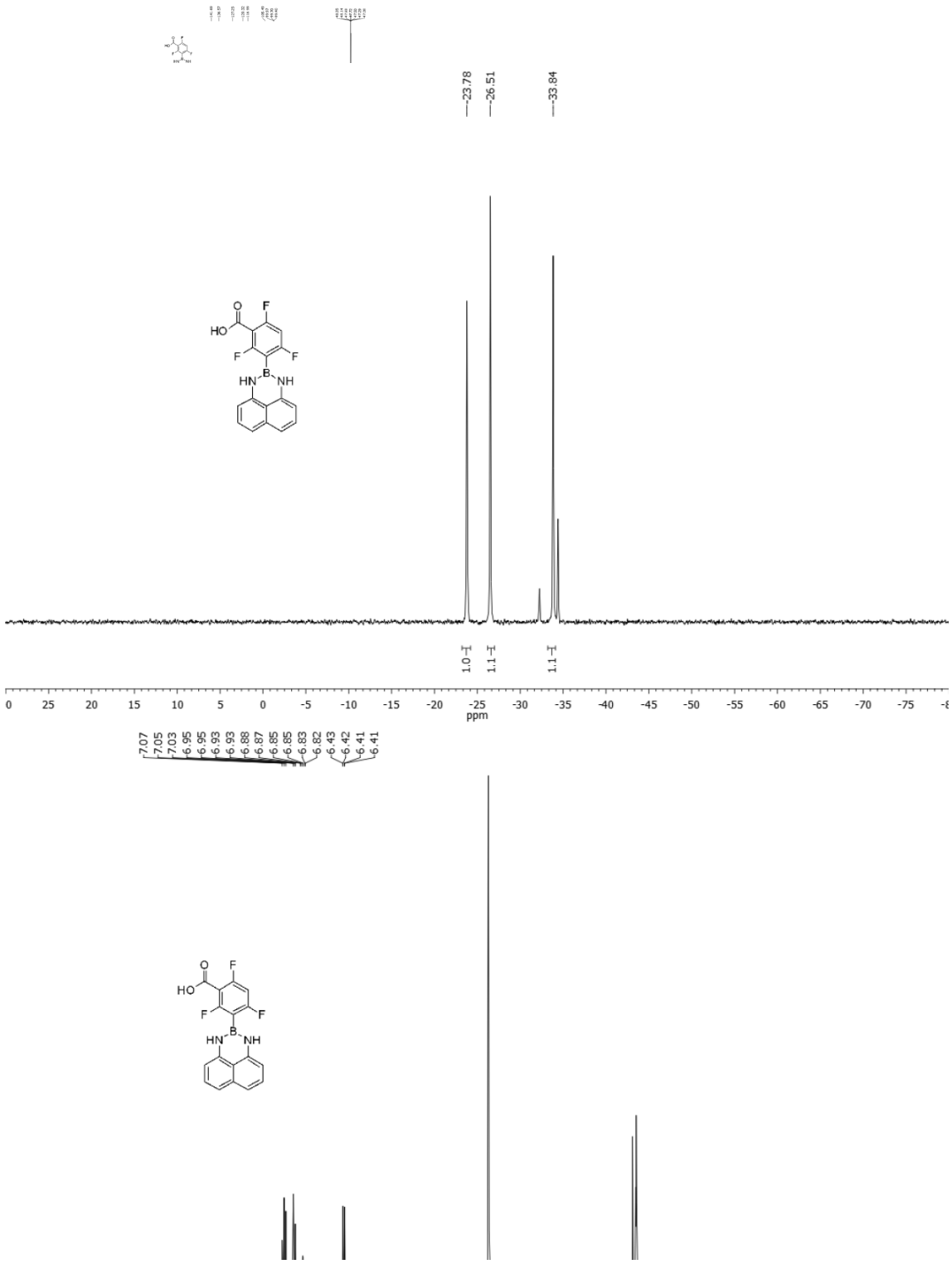
-23.78
-26.51
-33.84
1.0
1.1
1.1
ppm
7.07
7.05
7.03
6.95
6.95
6.93
6.93
6.88
6.87
6.85
6.85
6.83
6.82
6.43
6.42
6.41
6.41

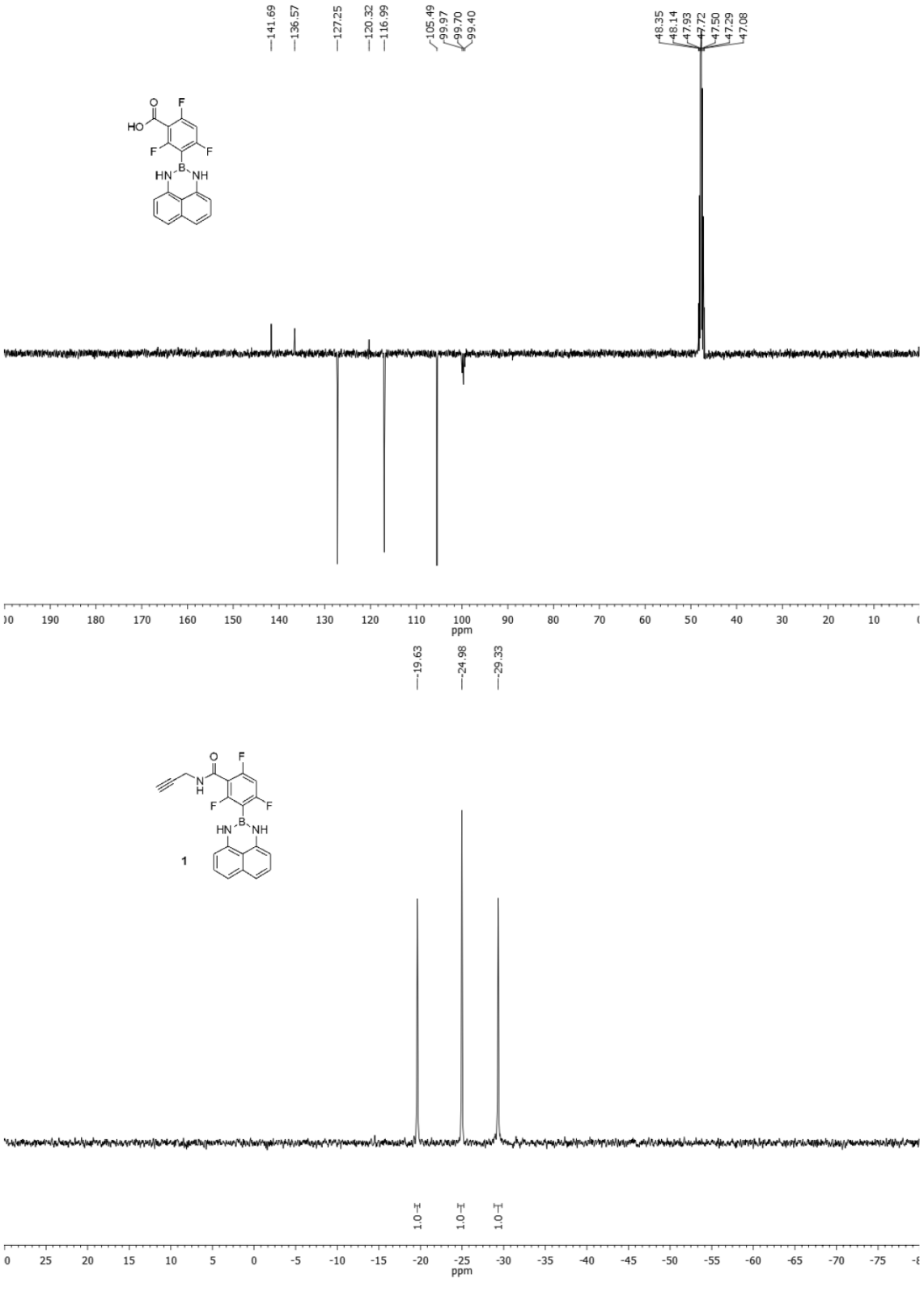
141.69
136.57
127.25
120.32
116.99
105.49
99.97
99.70
99.40
48.35
48.14
47.93
47.72
47.50
47.29
47.08
ppm
-19.63
-24.98
-29.33
1
1.0
1.0
1.0
ppm

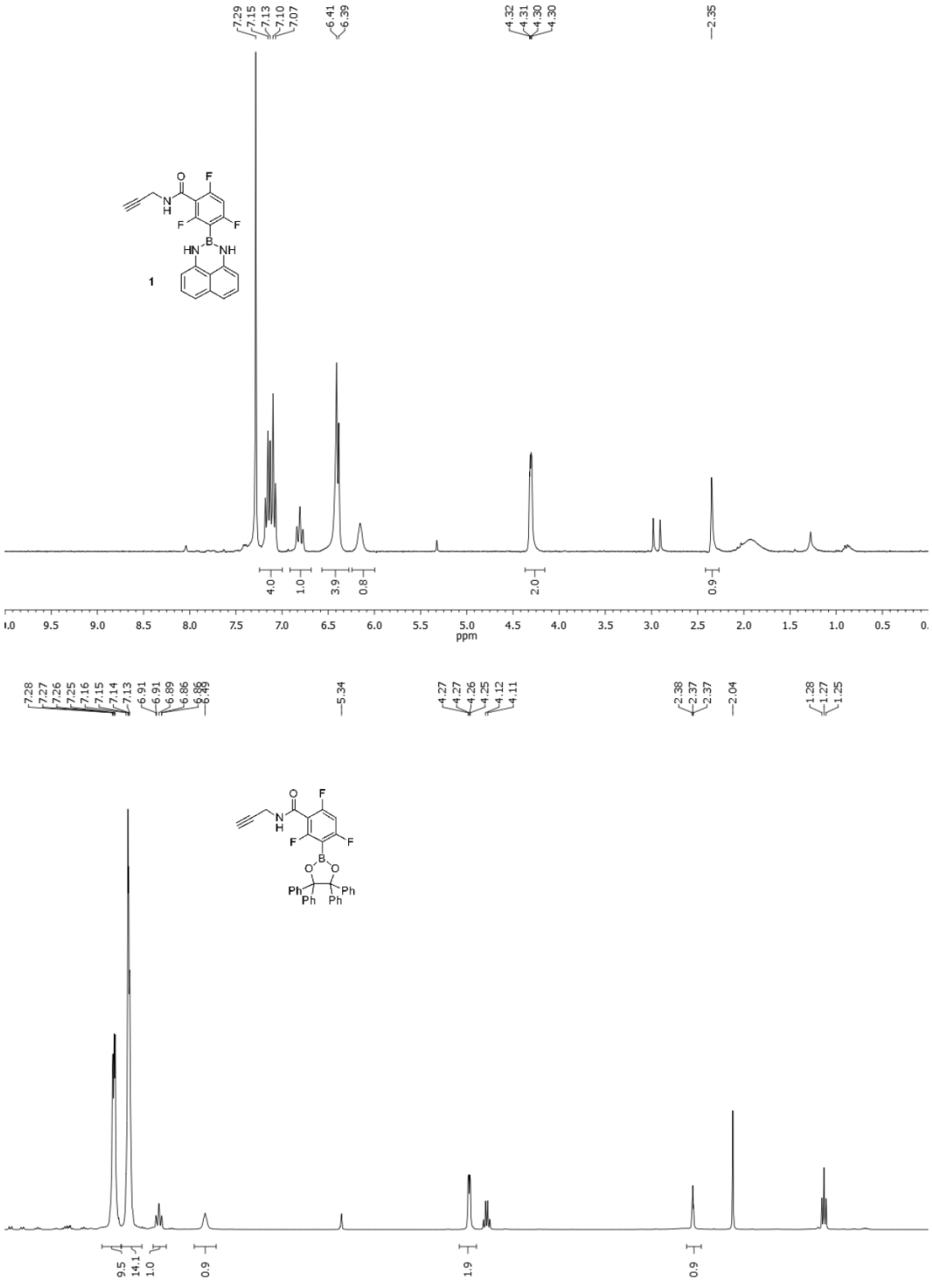
7.29
7.15
7.13
7.10
7.07
6.41
6.39
4.32
4.31
4.30
4.30
2.35
1
4.0
1.0
3.9
0.8
2.0
0.9
ppm
7.28
7.27
7.26
7.25
7.16
7.15
7.14
7.13
6.91
6.91
6.89
6.86
6.86
6.85
5.34
4.27
4.27
4.26
4.25
4.12
4.11
2.38
2.37
2.37
2.04
1.28
1.27
1.25
Ph
Ph
Ph
Ph
9.5
14.1
1.0
0.9
1.9
0.9

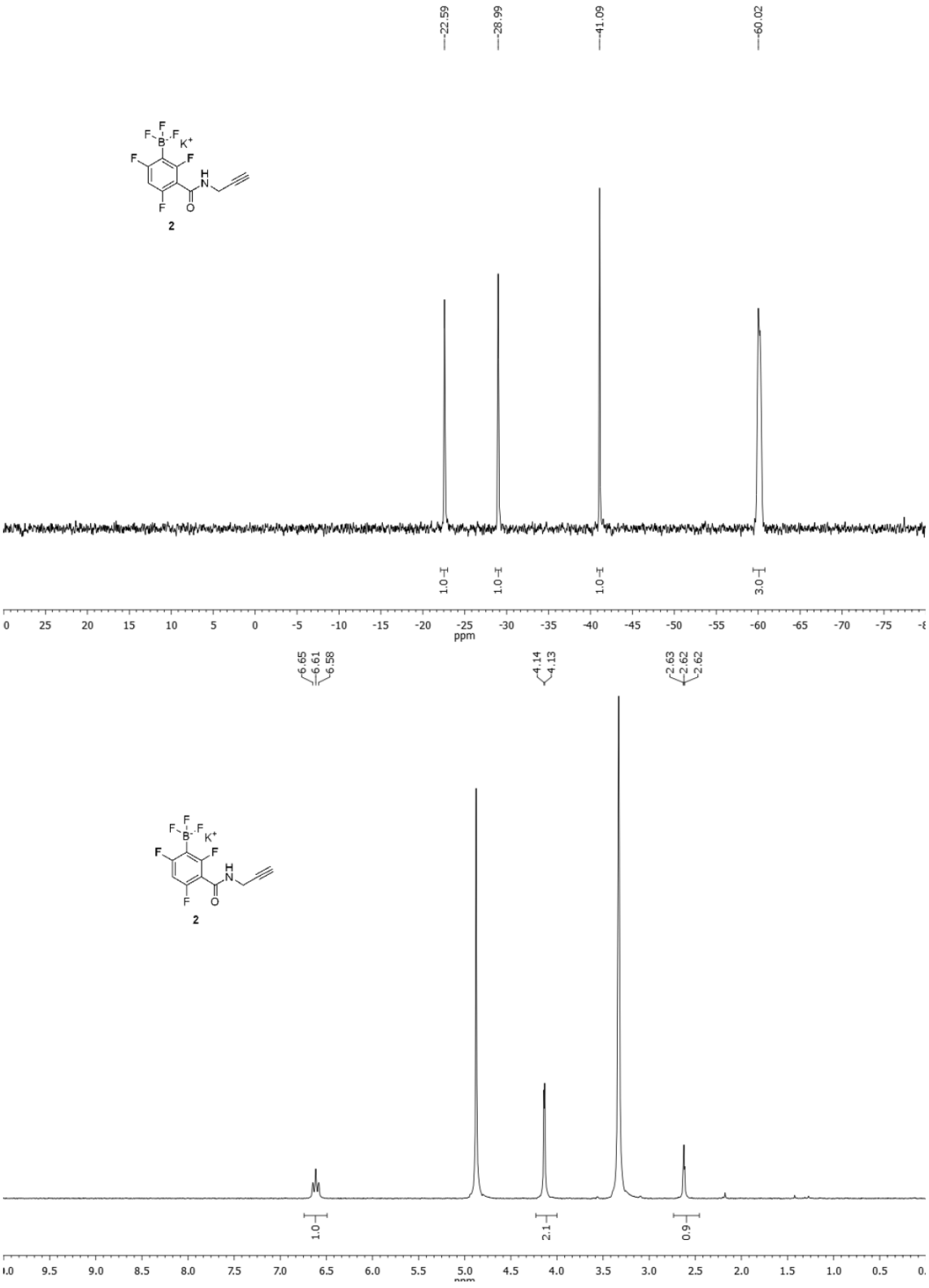
-22.59
-28.99
-41.09
-60.02
1.0
1.0
1.0
3.0
ppm
6.65
6.61
6.58
4.14
4.13
2.63
2.62
2.62
1.0
2.1
0.9
2